

Hypothalamic POMC neurons promote cannabinoid-induced feeding

Marco Koch^{1,2}, Luis Varela¹, Jae Geun Kim^{1†}, Jung Dae Kim^{1,3}, Francisco Hernández-Nuño¹, Stephanie E. Simonds⁴, Carlos M. Castorena⁵, Claudia R. Vianna⁵, Joel K. Elmquist⁵, Yury M. Morozov⁶, Pasko Rakic^{6,7}, Ingo Bechmann², Michael A. Cowley⁴, Klara Szigeti-Buck¹, Marcelo O. Dietrich^{1,6}, Xiao-Bing Gao¹, Sabrina Diano^{1,3,6} & Tamas L. Horvath^{1,3,6,7}

Hypothalamic pro-opiomelanocortin (POMC) neurons promote satiety. Cannabinoid receptor 1 (CB₁R) is critical for the central regulation of food intake. Here we test whether CB₁R-controlled feeding in sated mice is paralleled by decreased activity of POMC neurons. We show that chemical promotion of CB₁R activity increases feeding, and notably, CB₁R activation also promotes neuronal activity of POMC cells. This paradoxical increase in POMC activity was crucial for CB₁R-induced feeding, because designer-receptors-exclusively-activated-by-designer-drugs (DREADD)-mediated inhibition of POMC neurons diminishes, whereas DREADD-mediated activation of POMC neurons enhances CB₁R-driven feeding. The *Pomc* gene encodes both the anorexigenic peptide α -melanocyte-stimulating hormone, and the opioid peptide β -endorphin. CB₁R activation selectively increases β -endorphin but not α -melanocyte-stimulating hormone release in the hypothalamus, and systemic or hypothalamic administration of the opioid receptor antagonist naloxone blocks acute CB₁R-induced feeding. These processes involve mitochondrial adaptations that, when blocked, abolish CB₁R-induced cellular responses and feeding. Together, these results uncover a previously unsuspected role of POMC neurons in the promotion of feeding by cannabinoids.

Feeding behaviour is under the control of hypothalamic circuits¹. In the hypothalamic arcuate nucleus (ARC), Agouti-related peptide (AgRP)-expressing neurons, when activated, promote food intake^{2,3}, whereas POMC-producing neurons promote satiety⁴. Homeostatic feeding regulation can be disrupted by exogenous substances, such as cannabinoids⁵. Activation of CB₁R can lead to robust feeding despite animals being sated⁶. However, the role of cannabinoids in the control of hypothalamic feeding circuits remains enigmatic^{5–10}. In this study, we interrogated whether CB₁R-mediated feeding in a satiety state is associated with suppressed activity of POMC neurons, and if so, whether the altered activity of these neurons is important for CB₁R-induced feeding.

CB₁R drives activation of POMC neurons

We found that the selective CB₁R agonist arachidonyl-2'-chloroethylamide (ACEA) induced a known¹¹ bimodal feeding response in fed mice (Extended Data Fig. 1a–c). Notably, hyperphagic stimulation of CB₁R resulted in activation of POMC neurons, as assessed by expression of the proto-oncogene cFOS (Fig. 1A, B). *Ex vivo* electrophysiological recordings from ACEA-treated mice confirmed POMC neuronal activation (Fig. 1C). Next, we analysed slices acutely treated with ACEA. In the presence of tetrodotoxin (TTX), which blocks action potentials, ACEA failed to directly alter the membrane current of POMC neurons (Fig. 1D, a). We found that without TTX, low doses of ACEA (200 nM) induced depolarization of POMC neurons (Fig. 1D, b), as reported earlier¹², whereas high ACEA doses (1 μ M) resulted in hyperpolarization of POMC cells (Fig. 1D, c). As an anatomical substrate of these effects, we detected CB₁R immunolabelling in both GABAergic and glutamatergic presynaptic terminals of POMC neurons (Fig. 1D, d). In line with these findings, hyperphagic doses of CB₁R agonists ACEA or

WIN-55,212-2 mesylate (hereafter referred to as WIN) (1 mg kg⁻¹ body weight) induced cFOS expression in POMC neurons (Fig. 1E). By contrast, the ACEA dose that did not affect food intake (5 mg kg⁻¹ body weight) also did not induce cFOS expression in POMC neurons (Fig. 1E).

ACEA injected into the ARC resulted in a feeding response similar to that seen after its peripheral injection (Extended Data Fig. 1d). This local ACEA injection also activated POMC neurons as assessed by expression of phosphorylated CREB (pCREB(Ser 133)) and cFOS immunolabelling (Fig. 1F, G). Administration of the inverse CB₁R agonist rimonabant (RIMO) into the ARC blocked stimulation of food intake by peripheral ACEA application (Extended Data Fig. 1e–g), and, RIMO-mediated CB₁R blockade augmented the inactivation of POMC neurons in fasted mice as assessed by cFOS expression (Fig. 1H, I and Extended Data Fig. 1h).

POMC neurons drive feeding by cannabinoids

To determine whether the paradoxical POMC neuronal activation triggered by CB₁R is relevant for feeding, we injected inhibitory or stimulatory DREADD (AAV-hM4Di-mCherry or AAV-hM3Dq-mCherry³) into the ARC of *Pomc-Cre* mice (Extended Data Fig. 2a, b).

Clozapine-N-oxide (CNO)-driven activation of inhibitory DREADD reduced the numbers of cFOS-immunolabelled neurons in the ARC (Extended Data Fig. 2c), and blocked ACEA-induced activation of POMC neurons in fed mice (Extended Data Fig. 2d, e). CNO-mediated inhibition of POMC neurons in vehicle-treated mice enhanced feeding 8 h after CNO administration (Extended Data Fig. 2f). Conversely, DREADD-mediated activation of POMC neurons in vehicle-treated mice suppressed feeding 8 h after CNO application (Extended Data

¹Program in Integrative Cell Signaling and Neurobiology of Metabolism, Section of Comparative Medicine, Yale University School of Medicine, New Haven, Connecticut 06520, USA. ²Institute of Anatomy, University of Leipzig, 04103 Leipzig, Germany. ³Department of Obstetrics, Gynecology and Reproductive Sciences, Yale University School of Medicine, New Haven, Connecticut 06520, USA. ⁴Obesity & Diabetes Institute, Department of Physiology, Monash University, Clayton, Victoria 3800, Australia. ⁵Division of Endocrinology & Metabolism, Department of Internal Medicine, The University of Texas Southwestern Medical Center, Dallas, Texas 75390, USA. ⁶Department of Neurobiology, Yale University School of Medicine, New Haven, Connecticut 06520, USA. ⁷Kavli Institute for Neuroscience, Yale University School of Medicine, New Haven, Connecticut 06520, USA. †Present address: Division of Life Sciences, College of Life Sciences and Bioengineering, Incheon National University, Incheon 406-772, South Korea.

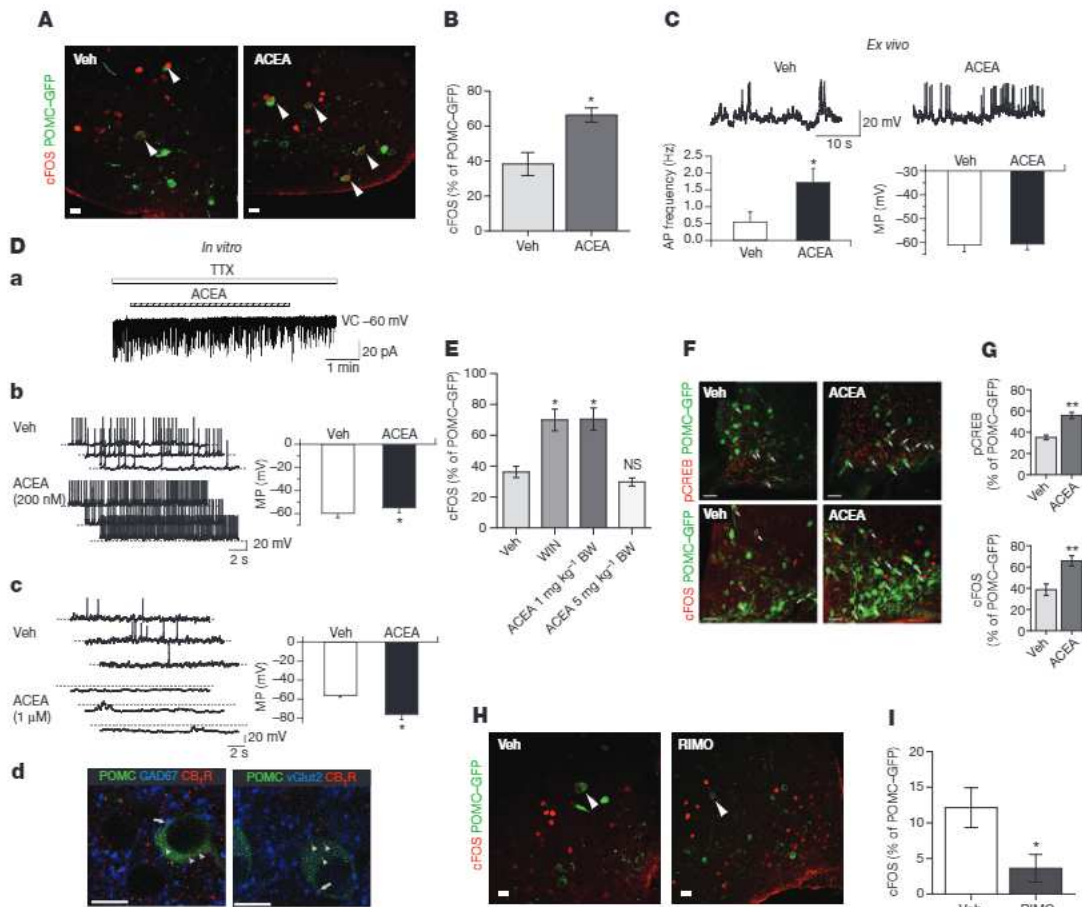


Figure 1 | CB₁R-driven paradoxical POMC activation. **A, B**, In fed mice, ACEA increased cFOS expression in POMC neurons (vehicle (Veh), $n = 5$ mice, $38.3 \pm 6.6\%$; ACEA, $n = 4$, $66.4 \pm 4.1\%$; $*P < 0.05$). GFP, green fluorescent protein. **C**, In the fed state, ACEA increased POMC action potential (AP) frequency (left, vehicle, $n = 22$ cells per 7 mice, 0.56 ± 0.29 Hz; ACEA, $n = 22/7$, 1.73 ± 0.4 Hz; $*P < 0.05$; seven independent experiments using litters from different parents). ACEA failed to alter POMC membrane potential (MP) (right, vehicle, -61.1 ± 2.7 mV; ACEA, -60.7 ± 2.3 mV). **D, a**, In the presence of TTX, 1 μ M ACEA failed to alter POMC membrane current (4 out of 4 cells). VC, voltage clamp. **D, b**, Without TTX, 200 nM ACEA depolarized POMC neurons (vehicle, $n = 6$ cells per 3 mice, -59.8 ± 3.7 mV; ACEA, $n = 6/3$, -55.0 ± 4.2 mV; $*P < 0.05$; three independent experiments). **D, c**, In the absence of TTX, a high ACEA dose (1 μ M) hyperpolarized POMC neurons (vehicle, $n = 6$ cells per 4 mice, -56.2 ± 1.6 mV; ACEA, $n = 6/4$, -76.1 ± 5.1 mV; $*P < 0.05$; four independent experiments). **D, d**, Arrows: CB₁R immunolabelling (red) in GABAergic (blue, left) and glutamatergic (blue, right) presynaptic terminals of POMC-GFP neurons (green). Arrowheads: POMC-GFP CB₁R immunolabelling (images are representative of three

independent experiments). **E**, Increased cFOS expression in POMC neurons by hyperphagic but not neutral CB₁R activation (vehicle, $n = 3$ mice, $36.3 \pm 3.6\%$; WIN, $n = 4$, $69.9 \pm 7\%$; 1 mg kg⁻¹ body weight (BW) ACEA, $n = 3$, $70.4 \pm 7.2\%$; 5 mg kg⁻¹ body weight ACEA, $n = 3$, $29.8 \pm 2.6\%$; $*P < 0.05$ versus vehicle (one-way analysis of variance (ANOVA) followed by Dunnett's multiple comparisons test). NS, not significant ($P > 0.05$). **F, G**, Local ARC hyperphagic CB₁R activation induced pCREB(Ser 133) (vehicle, $n = 4$ mice, $35.2 \pm 2.2\%$; ACEA, $n = 5$, $55.8 \pm 3\%$) and cFOS (vehicle, $n = 5$, $38.7 \pm 5.4\%$; ACEA, $n = 5$, $65.8 \pm 4.8\%$; $**P < 0.01$) expression in POMC cells. **H, I**, In the fasted state, RIMO decreased POMC cFOS expression (vehicle, $n = 6$ mice, $12.1 \pm 2.8\%$; RIMO, $n = 6$, $3.6 \pm 1.9\%$; $*P < 0.05$; two independent experiments). All values (biological replicates: **A, B, D, d, E-I**; biological replicates including technical replicates: **C, D, a-c**) denote mean \pm s.e.m. POMC cFOS expression analyses in fed mice were performed in three independent experiments using litters from different parents (**A, B, E-G**). P values (unpaired comparisons) by two-tailed Student's t -test, unless otherwise stated. Scale bars, 25 μ m (**A, D, d, H**) and 50 μ m (**F**).

Fig. 2g). These findings are in line with previous observations that ARC POMC neurons gradually suppress feeding behaviour^{4,13}. By contrast, DREADD-induced inhibition of POMC neurons significantly reduced acute, cannabinoid (WIN or ACEA)-induced feeding (Fig. 2a–d), whereas the acute hyperphagic response to the CB₁R agonist ACEA was significantly amplified by DREADD-induced activation of POMC neurons (Fig. 2e, f). Thus, our results demonstrate that POMC neuronal activation is key for feeding evoked by CB₁R in sated mice.

CB₁R drives β -endorphin but not α -MSH release

The *Pomc* gene encodes both the anorexigenic peptide α -melanocyte-stimulating hormone (α -MSH) and the opioid peptide β -endorphin, which can be orexigenic^{14–16}. The hypothalamic paraventricular nucleus (PVN) is the main site where efferents of POMC neurons are thought to affect feeding^{1,17,18}. ACEA-mediated activation of CB₁R did not affect

α -MSH levels (Extended Data Fig. 3a–d, i and Extended Data Table 1a), but it was correlated with increased β -endorphin levels in the PVN⁷ (Extended Data Fig. 3e–h, j and Extended Data Table 1b). In line with this, ACEA triggered the secretion of β -endorphin but not α -MSH into the supernatant of acute mediobasal hypothalamic explants derived from fed mice (Fig. 3a).

Next, we blocked CB₁R in the ARC by local injection of RIMO, which diminished ACEA-induced β -endorphin secretion (Fig. 3b). ACEA-induced β -endorphin secretion was absent in CB₁R knockout (*Cnr1*^{-/-}) mice (Fig. 3b). ACEA affected β -endorphin levels in a dose-dependent manner (Extended Data Fig. 4a and Extended Data Table 2), and local injection of ACEA into the ARC robustly induced β -endorphin levels in the PVN (Extended Data Fig. 4b, c and Extended Data Table 3).

α -MSH and β -endorphin are derived from POMC by pro-protein convertases, including PC-1 and PC-2 (ref. 14). CB₁R activation did

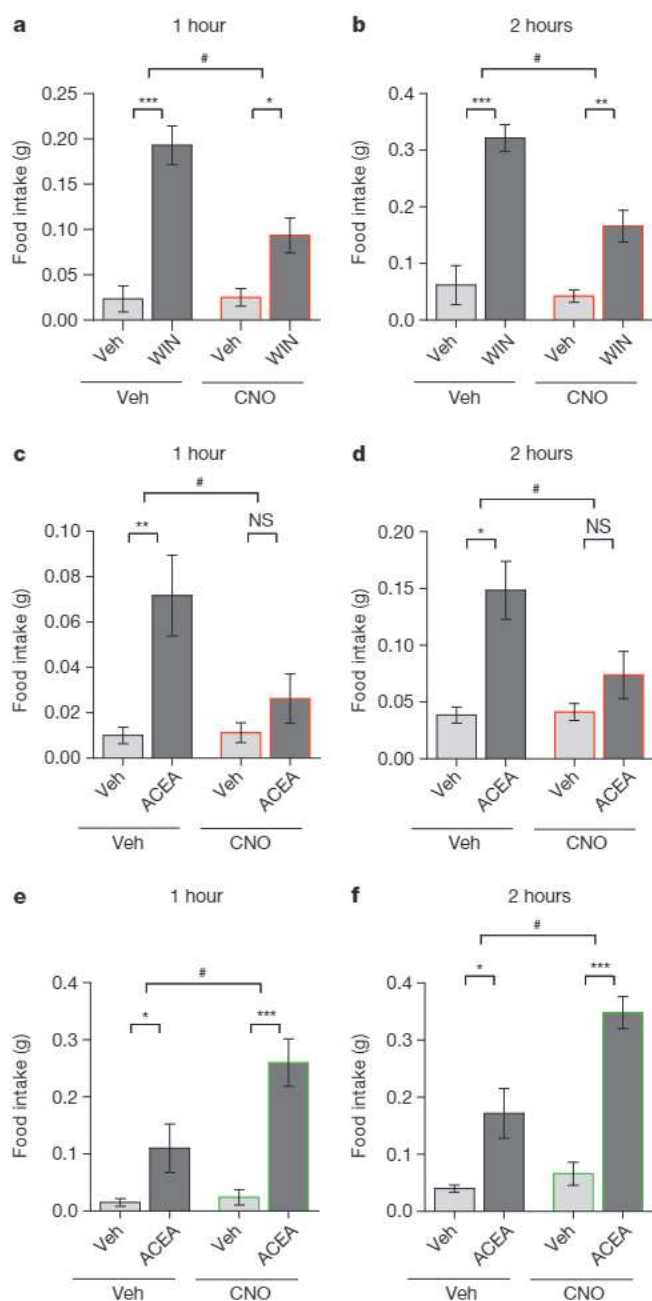


Figure 2 | DREADD-controlled POMC activity interferes with cannabinoid-induced feeding. **a, b**, DREADD-driven POMC inhibition reduced WIN-mediated hyperphagia, 1 h (**a**) and 2 h (**b**) after injection (**a**, 1 h: vehicle plus vehicle, $n = 6$ mice, 0.02 ± 0.01 ; vehicle plus WIN, $n = 13$, 0.19 ± 0.02 ; CNO plus vehicle, $n = 8$, 0.03 ± 0.01 ; CNO plus WIN, $n = 12$, 0.09 ± 0.02 ; **b**, 2 h: vehicle plus vehicle, 0.06 ± 0.03 ; vehicle plus WIN, 0.32 ± 0.02 ; CNO plus vehicle, 0.04 ± 0.01 ; CNO plus WIN, 0.17 ± 0.03 ; two independent experiments). **c, d**, DREADD-driven POMC inhibition blocked ACEA-mediated hyperphagia, 1 h (**c**) and 2 h (**d**) after injection (**c**, 1 h: vehicle plus vehicle, $n = 6$, 0.01 ± 0.004 ; vehicle plus ACEA, $n = 6$, 0.07 ± 0.02 ; CNO plus vehicle, $n = 8$, 0.01 ± 0.004 ; CNO plus ACEA, $n = 8$, 0.03 ± 0.01 ; **d**, 2 h: vehicle plus vehicle, 0.04 ± 0.01 ; vehicle plus ACEA, 0.15 ± 0.03 ; CNO plus vehicle, 0.04 ± 0.01 ; CNO plus ACEA, 0.07 ± 0.02 ; two independent experiments). **e, f**, DREADD-driven POMC activation enhanced ACEA-mediated hyperphagia, 1 h (**e**) and 2 h (**f**) after injection (**e**, 1 h: vehicle plus vehicle, $n = 6$, 0.02 ± 0.01 ; vehicle plus ACEA, $n = 6$, 0.11 ± 0.04 ; CNO plus vehicle, $n = 5$, 0.02 ± 0.01 ; CNO plus ACEA, $n = 5$, 0.26 ± 0.04 ; **f**, 2 h: vehicle plus vehicle, 0.04 ± 0.01 ; vehicle plus ACEA, 0.17 ± 0.04 ; CNO plus vehicle, 0.07 ± 0.02 ; CNO plus ACEA, 0.35 ± 0.03). All values (biological replicates) denote mean \pm s.e.m. Five independent experiments using litters from different parents. * $P < 0.05$, ** $P < 0.01$, *** $P < 0.001$, # $P < 0.05$ interaction of WIN or ACEA and CNO (two-way ANOVA, followed by Sidák's multiple comparisons test).

diminished CB₁R-dependent hyperphagic response of WIN (Fig. 3g) and ACEA (Fig. 3h). Central application of naloxone into the PVN also diminished ACEA- and WIN-evoked hyperphagia (Fig. 3i).

β -endorphin was shown to be a feed-forward presynaptic inhibitor of AgRP neuronal activity⁹. In line with this, 90 min after ACEA application, the action potential frequency of AgRP neurons was decreased (Fig. 3j).

Taken together, we conclude that CB₁R-induced acute feeding in sated mice is evoked by POMC neurons via β -endorphin release and μ -opioid receptor activation while AgRP neurons are silenced.

CB₁R induces mitochondrial adaptations

Next we explored intracellular mechanisms that may bring about changes in neuropeptide release properties of POMC cells. Real-time PCR revealed local ARC CB₁R (*Cnr1*) expression (Fig. 4a). Immunolabelling for CB₁R showed both presynaptic and intracellular localization of CB₁R in POMC neurons (Fig. 4b, c). Electron microscopy revealed the presence of CB₁R immunoreactivity in mitochondria of POMC cells (Fig. 4d and Extended Data Fig. 5e), a finding consistent with previous observations of CB₁R in mitochondria of neurons^{21–25}. Dynamic changes of mitochondria–endoplasmic-reticulum (ER) contacts were shown in POMC neurons in association with changes in their activity and metabolic milieu^{26,27}. In line with this, we found that hyperphagic activation of CB₁R resulted in an increased number of mitochondria–ER contacts (Fig. 4e–g). We also observed that ACEA-mediated activation of CB₁R dose-dependently increased hypothalamic coupled (state 3) and uncoupled (state 4) mitochondrial respiration (Fig. 4h–j). Increased coupled mitochondrial respiration is associated with increased generation of reactive oxygen species (ROS), which we showed previously to increase POMC neuronal activity²⁸. Indeed, we found that hyperphagic ACEA administration increased ROS levels in POMC neurons (Fig. 5a, b).

CB₁R-induced energetic switch relies on UCP2

ROS are known to induce the expression and function of mitochondrial uncoupling protein 2 (UCP2)^{29,30}, a regulator of hypothalamic mitochondrial respiration and feeding^{31,32}. Hyperphagic activation of CB₁R by ACEA increased hypothalamic expression of *Ucp2* messenger RNA (Fig. 5c). ACEA failed to alter mitochondrial respiration in the hypothalamus of UCP2 knockout mice (*Ucp2*^{−/−}; Fig. 5d). CB₁R-induced changes in POMC, PC-1 and PC-2 were diminished in *Ucp2*^{−/−} mice (Fig. 5e–g and Extended Data Fig. 6c). Whereas CB₁R-driven POMC neuronal activation was partially retained (Fig. 5h), neither CB₁R-associated feeding (Fig. 5i) nor CB₁R-dependent increase of β -endorphin (Fig. 5j and Extended Data Table 4) was observable in *Ucp2*^{−/−} mice.

not affect transcriptional regulation of either of these convertases (*Pcsk1* and *Pcsk2*, respectively; Extended Data Fig. 5a, b), but it did increase protein levels of PC-1 and PC-2 (Fig. 3c, d and Extended Data Fig. 5c).

Differential release dynamics of β -endorphin and α -MSH suggest that they may be present in non-overlapping intracellular compartments of POMC neurons. We observed that immunolabelling of these peptides did not overlap in $33.5 \pm 4.6\%$ (mean \pm s.e.m.) of POMC boutons in the PVN (Fig. 3e). With electron microscopy, we confirmed that β -endorphin and α -MSH could be found in separate vesicles within the same neuronal profile of the PVN (Fig. 3f). Thus, our data indicate that separate vesicle pools of β -endorphin and α -MSH are under diverse regulatory mechanisms.

Naloxone blocks cannabinoid-induced feeding

Previous findings showed that local infusion of β -endorphin into the PVN could induce hyperphagia^{19,20}. In fed mice, the μ -opioid receptor antagonist naloxone (NALO; 7.5 mg kg^{−1} body weight, intraperitoneal)

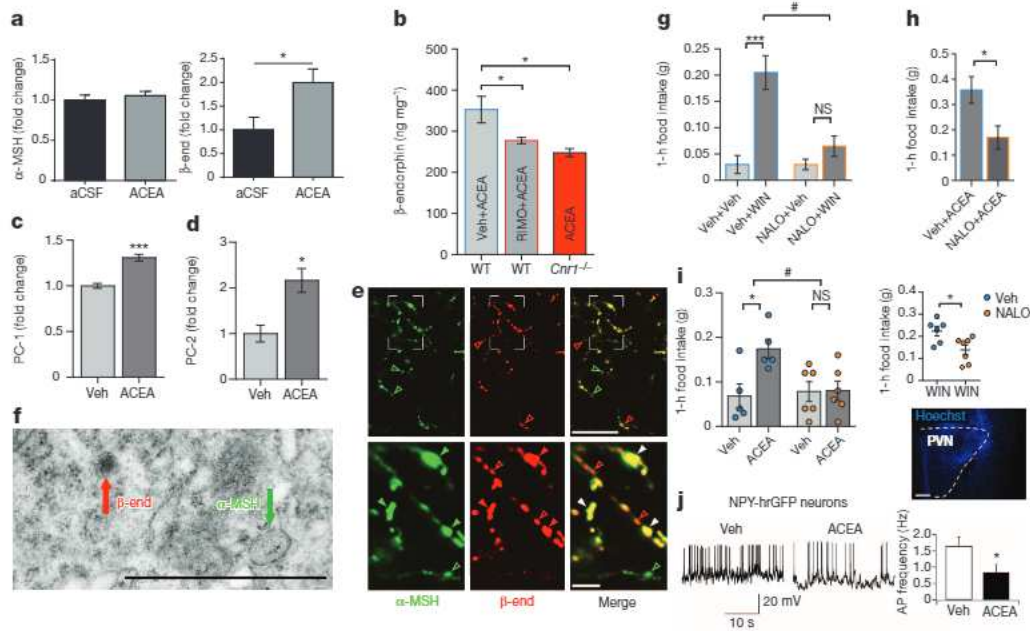


Figure 3 | CB₁R triggers hypothalamic β -endorphin release and drives feeding via opioid receptors. **a**, ACEA did not affect *in vitro* α -MSH secretion (artificial cerebrospinal fluid (aCSF), $n = 13$ mice, 1.00 ± 0.06 ; ACEA, $n = 6$, 1.05 ± 0.05 ; $P > 0.05$) but increased β -endorphin (β -end) release (aCSF, $n = 9$, 1.00 ± 0.27 ; ACEA, $n = 4$, 2.00 ± 0.29 ; $*P < 0.05$). **b**, ARC administration of RIMO blocked ACEA-induced increase of β -endorphin as measured by ELISA in wild-type (WT) mice (vehicle plus ACEA, $n = 6$ mice, 352.7 ± 32.4 ; RIMO plus ACEA, $n = 6$, 277.4 ± 7.5 ; $*P < 0.05$ versus vehicle plus ACEA). ACEA did not increase β -endorphin in CB₁R knockout (*Cnr1*^{-/-}) mice ($n = 4$, 247.8 ± 9.9 ; $*P < 0.05$, one-way ANOVA, followed by Dunnett's multiple comparisons test). **c**, **d**, ACEA increased hypothalamic PC-1 (**c**) and PC-2 (**d**) protein levels (all groups $n = 4$ mice; PC-1: vehicle, 1.00 ± 0.03 ; ACEA, 1.31 ± 0.04 ; $***P < 0.001$; PC-2: vehicle, 1.00 ± 0.18 ; ACEA, 2.16 ± 0.26 ; $*P < 0.05$). **e**, Overview (top) and magnification (bottom) of α -MSH (green) and β -endorphin (red) in POMC fibres in the PVN. Coloured arrows indicate non-overlapping immunolabelling (images are representative of three independent experiments). **f**, Electron micrograph showing peroxidase immunolabelling of β -endorphin (red arrow) and immunogold labelling of α -MSH (green arrow) in different vesicles of the same process (images are representative of three independent experiments). **g**, **h**, Peripheral administration of NALO (7.5 mg kg^{-1} body weight, intraperitoneal) blocked hyperphagia induced by WIN (**g**; vehicle plus vehicle, $n = 10$ mice, 0.03 ± 0.02 ;

vehicle plus WIN, $n = 10$, 0.21 ± 0.03 ; NALO plus vehicle, $n = 8$, 0.03 ± 0.01 , NALO plus WIN, $n = 10$, 0.07 ± 0.02 ; $***P < 0.001$, $\#P < 0.05$ for interaction of NALO and WIN; two-way ANOVA followed by Šidák's multiple comparisons test; two independent experiments) or induced by ACEA (**h**; vehicle plus ACEA, $n = 4$, 0.36 ± 0.05 ; NALO plus ACEA, $n = 4$, 0.17 ± 0.05 ; $*P < 0.05$). **i**, PVN NALO application ($5 \mu\text{g per } 0.5 \mu\text{l}$) blocked hyperphagia induced by ACEA (intraperitoneal; vehicle plus vehicle, $n = 5$, 0.07 ± 0.03 ; vehicle plus ACEA, $n = 5$, 0.17 ± 0.02 ; NALO plus VEH, $n = 6$, 0.08 ± 0.02 ; NALO plus ACEA, $n = 6$, 0.08 ± 0.02 ; $*P < 0.05$, $\#P < 0.05$ for interaction of NALO and ACEA; two-way ANOVA, followed by Šidák's multiple comparisons test; two independent experiments) or induced by WIN (intraperitoneal; vehicle plus WIN, $n = 6$, 0.22 ± 0.02 ; NALO plus WIN, $n = 7$, 0.14 ± 0.02 ; $*P < 0.05$; Hoechst (blue) injection for verification of correct cannula placement). **j**, Hyperphagic ACEA decreased AgRP/NPY-hrGFP (NPY-hrGFP) action potential (AP) frequency (vehicle, $n = 20$ cells per 6 mice, $1.65 \pm 0.27 \text{ Hz}$; ACEA, $n = 20/6$, $0.84 \pm 0.24 \text{ Hz}$; $*P < 0.05$; six independent experiments using litters from different parents). All values (biological replicates: **a–i**; biological replicates including technical replicates: **j**) denote mean \pm s.e.m. P values (unpaired comparisons) by two-tailed Student's t -test, unless stated otherwise. Scale bars, $25 \mu\text{m}$ (**e**, top), $5 \mu\text{m}$ (**e**, bottom), $1 \mu\text{m}$ (**f**) and $25 \mu\text{m}$ (**i**).

Thus, we conclude that UCP2 has a critical role in mediating CB₁R action on intracellular adaptation of POMC neurons while promoting feeding.

Discussion

Since the discovery of the melanocortin system and its satiety promoting action via melanocortin 4 receptors^{33–35}, POMC neurons have been considered as key drivers of the cessation of feeding^{35–37}. However, our findings unmasked an overlooked, albeit previously proposed^{16,38} role for hypothalamic POMC neurons in the promotion of feeding. Specifically, we found that POMC neuronal activation is indispensable for appropriate promotion of feeding triggered by CB₁R activation in the state of satiety. This observation brings these neurons to a new light in feeding regulation.

Cannabinoid-controlled feeding behaviour is complex and probably relies on diverse modes of action^{11,39}. We focused on a specific action of cannabinoids, which is acute feeding evoked by CB₁R activation during the time of satiety. Thus, it is not unlikely that the cellular biological principles we uncovered here involving CB₁R action are not ubiquitous throughout the brain relating to cannabinoids. Nevertheless, the phenomenon of cannabis-triggered feeding in a state of satiety is a hallmark

of marijuana use in humans^{40,41}, and whether hypothalamic POMC neurons may be relevant to other aspect of the complex behavioural responses triggered by cannabis use will be important to address.

We found that cannabinoid-induced activation of POMC neurons and related feeding relies on both pre-synaptic modalities and mitochondrial mechanisms. Regarding the presynaptic events, it is intriguing to note that CB₁R activation had a bimodal effect, in which lower doses of the CB₁R agonist ACEA induced depolarization of POMC neurons, while higher doses hyperpolarized these cells. Because both GABAergic and glutamatergic pre-synaptic terminals on POMC neurons expressed CB₁R, it is reasonable to assume that the bimodal effect of cannabinoids on feeding are due to the differential sensitivity of GABAergic versus glutamatergic axons to CB₁R activation^{10,11}.

The effect of CB₁R on mitochondria, and the mitochondrial localization of CB₁R are both in line with the original observations on CB₁R action in other brain sites²³. In the present study, we showed that this CB₁R-dependent mitochondrial adaptation relies on the mitochondrial protein UCP2. UCP2 has been associated with hypothalamic feeding circuits^{31,42–44}, and was implicated in the malfunctioning of POMC neurons in diet-induced obesity⁴³. However, most of those studies tied UCP2 activity to lipid and glucose use of hypothalamic neurons³². Here, we

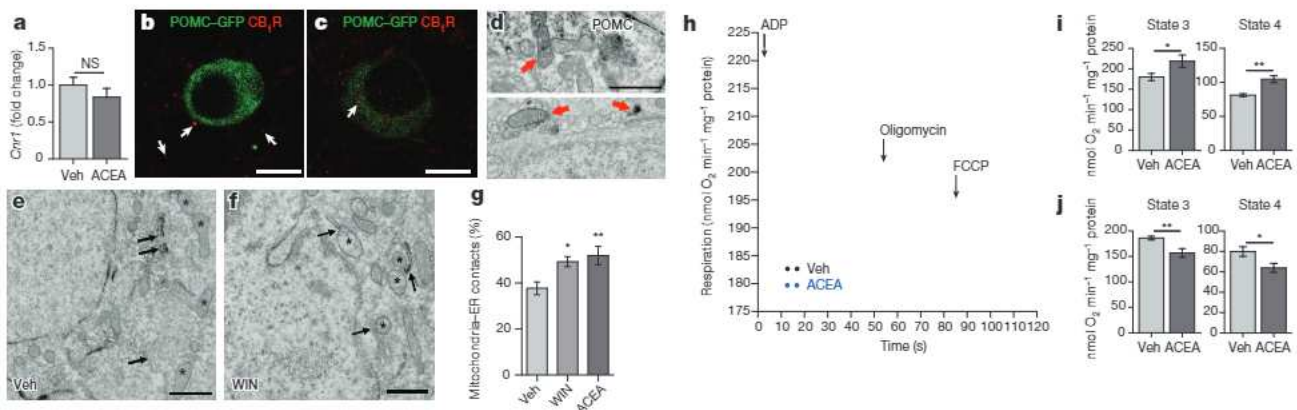


Figure 4 | CB₁R induces mitochondrial energetic switch in POMC neurons. **a**, ARC *Cnr1* mRNA expression (vehicle, $n = 5$ mice, 1.00 ± 0.11 ; ACEA, $n = 5$, 0.84 ± 0.12 ; $P > 0.05$). **b**, CB₁R (red; arrows) presynaptic to a POMC cell (GFP; green). **c**, **d**, Intracellular CB₁R in a POMC neuron (arrows). **d**, Mitochondrial CB₁R labelling (arrows) in POMC cell body (top) and process (bottom). Images are representative of three independent experiments. **e–g**, Increased mitochondria (stars)–ER (arrows) contacts in POMC neurons by WIN and ACEA (vehicle, $n = 10$ cells per 3 mice, 37.7 ± 2.8 ; WIN, $n = 10/3$, 49.3 ± 2.2 ; ACEA, $n = 10/3$, 51.9 ± 4 ; * $P < 0.05$, ** $P < 0.01$ versus vehicle; one-way ANOVA, followed by Dunnett's multiple comparisons test). **h**, **i**, Hyperphagic (1 mg kg^{-1} body weight) ACEA treatment increased

ex vivo hypothalamic mitochondrial respiration (state 3: vehicle, $n = 6$ mice, 180 ± 8.9 ; ACEA, $n = 8$, 218.9 ± 15 ; state 4: vehicle, 81.2 ± 2.1 ; ACEA, 104.7 ± 5 ; * $P < 0.05$, ** $P < 0.01$). **j**, Neutral dose of ACEA (5 mg kg^{-1} body weight) reduced mitochondrial respiration (state 3: vehicle, $n = 8$, 186.1 ± 3.7 ; ACEA, $n = 6$, 156.8 ± 8.4 ; state 4: vehicle, 79.9 ± 4.7 ; ACEA, 63.8 ± 4.4). Three independent experiments using litters from different parents (**h–j**). All values (biological replicates: **a–d**, **h–j**; biological replicates including technical replicates: **e–g**) denote mean \pm s.e.m. *P* values (unpaired comparisons) by two-tailed Student's *t*-test, unless stated otherwise. Scale bars, $25 \mu\text{m}$ (**b**, **c**), $0.5 \mu\text{m}$ (**d**) and $1 \mu\text{m}$ (**e**, **f**).

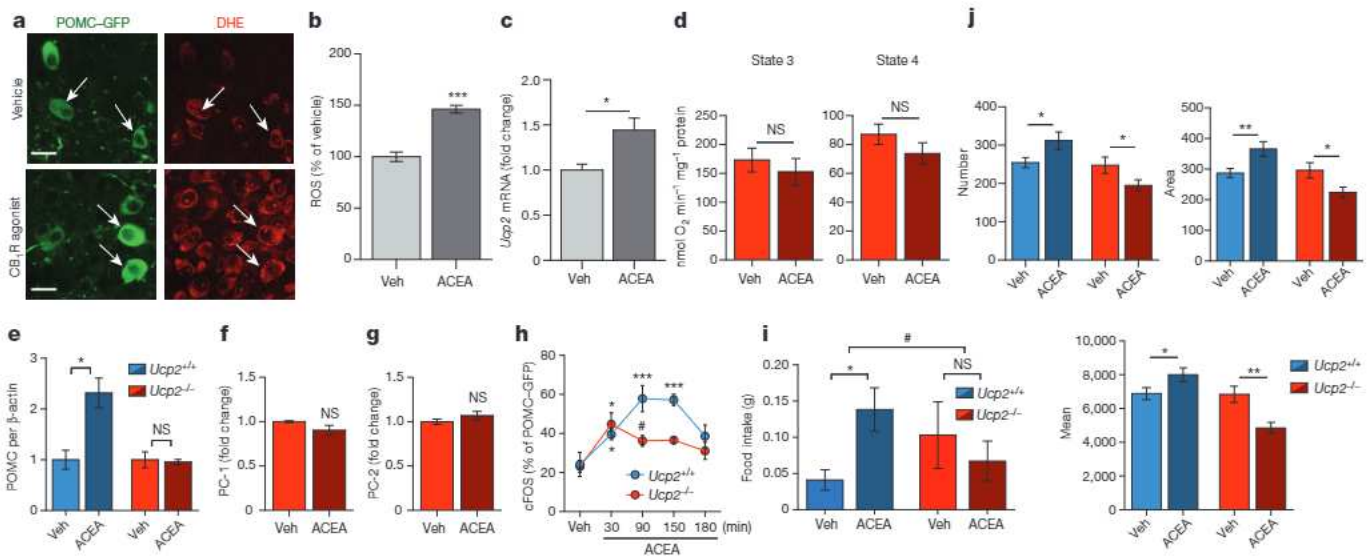


Figure 5 | CB₁R-induced energetic switch in POMC neurons relies on UCP2. **a**, **b**, ACEA increased POMC–GFP ROS (measured by dihydroethidium (DHE); vehicle, $n = 130$ cells per 7 mice, $100 \pm 4.5\%$; ACEA, $n = 248/9$, $146.2 \pm 3.7\%$; *** $P < 0.001$; three independent experiments). **c**, ACEA triggered hypothalamic *Ucp2* mRNA expression (vehicle, $n = 5$ mice, 1.00 ± 0.07 ; ACEA, $n = 5$, 1.44 ± 0.13 ; * $P < 0.05$). **d**, No effect of ACEA on *ex vivo* mitochondrial respiration in *Ucp2*^{−/−} mice (state 3: vehicle, $n = 3$ mice, 172.9 ± 20.6 ; ACEA, $n = 3$, 152.9 ± 22.9 ; state 4: vehicle, 87.1 ± 7.1 ; ACEA, 73.8 ± 7.5 ; $P > 0.05$). **e**, Increased POMC protein by ACEA in wild-type mice (vehicle, $n = 3$ mice, 1.00 ± 0.19 ; ACEA, $n = 3$, 2.3 ± 0.29 ; * $P < 0.05$) but not in *Ucp2*^{−/−} littermates (vehicle, $n = 3$, 1.00 ± 0.16 ; ACEA, $n = 3$, 0.96 ± 0.05 ; $P > 0.05$). **f**, **g**, No effect of ACEA on PC-1 protein (**f**) (vehicle, $n = 3$ mice, 1.00 ± 0.01 ; ACEA, $n = 4$, 0.9 ± 0.06 ; $P > 0.05$) or PC-2 protein (**g**) (vehicle, $n = 3$, 1.00 ± 0.03 ; ACEA, $n = 4$, 1.07 ± 0.05 ; $P > 0.05$) in *Ucp2*^{−/−} mice. **h**, cFOS expression in POMC neurons induced by ACEA in wild-type mice (vehicle, $n = 4$ mice, $22.1 \pm 6.2\%$; ACEA: 30 min, $n = 5$, $39.6 \pm 3\%$; 90 min, $n = 3$, $63.1 \pm 5.5\%$; 150 min, $n = 3$, $57.2 \pm 2.6\%$; 180 min, $n = 3$, $38.5 \pm 2.2\%$; * $P < 0.05$ versus vehicle, *** $P < 0.001$ versus vehicle; one-way ANOVA, followed by Dunnett's multiple comparisons test) and *Ucp2*^{−/−}

littermates (vehicle, $n = 6$ mice, $22.6 \pm 3.6\%$; ACEA: 30 min, $n = 6$, $42.2 \pm 6.4\%$; 90 min, $n = 6$, $36.6 \pm 3.1\%$; 150 min, $n = 3$, $37.3 \pm 1.6\%$; 180 min, $n = 3$, $33.5 \pm 5.2\%$; * $P < 0.05$ versus vehicle (one-way ANOVA, followed by Dunnett's multiple comparisons test); # $P < 0.05$ versus wild type 90-min ACEA (unpaired comparisons by multiple *t*-tests, followed by correction for multiple comparisons using Holm–Sidak's method). **i**, ACEA (2 h)-induced hyperphagia in wild-type mice (vehicle, $n = 10$ mice, 0.04 ± 0.01 g; ACEA, $n = 11$, 0.14 ± 0.03 g; * $P < 0.05$) but not in *Ucp2*^{−/−} littermates (vehicle, $n = 10$ mice, 0.1 ± 0.05 g; ACEA, $n = 14$, 0.07 ± 0.03 g; $P > 0.05$, # $P < 0.05$ for interaction between ACEA and genotypes; three independent experiments using litters from different parents). All values (biological replicates: **c–i**; biological replicates including technical replicates: **a**, **b**) denote mean \pm s.e.m. **j**, Increased PVN β -endorphin immunoreactivity in wild-type littermates (bilateral PVN analysis; vehicle, $n = 24$ values (technical replicates)/12 sections/4 mice (biological replicates); 90 min ACEA, $n = 24/12/4$); and reduced PVN β -endorphin immunoreactivity in *Ucp2*^{−/−} mice (vehicle, $n = 18/9/3$; ACEA, $n = 18/9/3$; see Extended Data Table 4 for values; * $P < 0.05$, ** $P < 0.01$). Values denote mean \pm s.e.m.

identified UCP2 mediation as being crucial for the switch from α -MSH to β -endorphin release by POMC neurons triggered by CB₁R activation. This suggests a novel function of UCPs in the central nervous system in which they control the release of specific vesicle pools of neuropeptides in POMC neurons. Whether this effect of UCP2 is specific to POMC cells or represents a novel regulatory principle for other neuronal populations that express UCP2, including the midbrain dopamine system⁴⁵, needs to be explored. It is well known that a single neuron can have the capability of generating and releasing different types of neuropeptides⁴⁶. How these different molecules with diverse functions are controlled within the same cells has not been fully resolved^{46,47}. Our findings raise the possibility that changes in mitochondrial functions may be critical regulators of these processes.

In summary, the overall effect of cannabinoids on feeding seems to be driven by both pre- and post-synaptic effects, which may be independent from one another, and it is their temporal synchrony that brings about the overall behavioural changes.

Online Content Methods, along with any additional Extended Data display items and Source Data, are available in the online version of the paper; references unique to these sections appear only in the online paper.

Received 22 March 2014; accepted 23 January 2015.

Published online 18 February 2015.

- Dietrich, M. O. & Horvath, T. L. Hypothalamic control of energy balance: insights into the role of synaptic plasticity. *Trends Neurosci.* **36**, 65–73 (2013).
- Aponte, Y., Atasoy, D. & Sternson, S. M. AGRP neurons are sufficient to orchestrate feeding behavior rapidly and without training. *Nature Neurosci.* **14**, 351–355 (2011).
- Krashes, M. J. *et al.* Rapid, reversible activation of AgRP neurons drives feeding behavior in mice. *J. Clin. Invest.* **121**, 1424–1428 (2011).
- Yang, Y., Atasoy, D., Su, H. H. & Sternson, S. M. Hunger states switch a flip-flop memory circuit via a synaptic AMPK-dependent positive feedback loop. *Cell* **146**, 992–1003 (2011).
- DiPatrizio, N. V. & Piomelli, D. The thrifty lipids: endocannabinoids and the neural control of energy conservation. *Trends Neurosci.* **35**, 403–411 (2012).
- Bermudez-Silva, F. J., Cardinal, P. & Cota, D. The role of the endocannabinoid system in the neuroendocrine regulation of energy balance. *J. Psychopharmacol.* **26**, 114–124 (2012).
- Sinnayah, P. *et al.* Feeding induced by cannabinoids is mediated independently of the melanocortin system. *PLoS ONE* **3**, e2202 (2008).
- Bakkali-Kassemi, L. *et al.* Effects of cannabinoids on neuropeptide Y and β -endorphin expression in the rat hypothalamic arcuate nucleus. *Br. J. Nutr.* **105**, 654–660 (2011).
- Ho, J., Cox, J. M. & Wagner, E. J. Cannabinoid-induced hyperphagia: correlation with inhibition of proopiomelanocortin neurons? *Physiol. Behav.* **92**, 507–519 (2007).
- Hentges, S. T., Low, M. J. & Williams, J. T. Differential regulation of synaptic inputs by constitutively released endocannabinoids and exogenous cannabinoids. *J. Neurosci.* **25**, 9746–9751 (2005).
- Bellochio, L. *et al.* Bimodal control of stimulated food intake by the endocannabinoid system. *Nature Neurosci.* **13**, 281–283 (2010).
- Hentges, S. T. Synaptic regulation of proopiomelanocortin neurons can occur distal to the arcuate nucleus. *J. Neurophysiol.* **97**, 3298–3304 (2007).
- Zhan, C. *et al.* Acute and long-term suppression of feeding behavior by POMC neurons in the brainstem and hypothalamus, respectively. *J. Neurosci.* **33**, 3624–3632 (2013).
- Dores, R. M. & Baron, A. J. Evolution of POMC: origin, phylogeny, posttranslational processing, and the melanocortins. *Ann. NY Acad. Sci.* **1220**, 34–48 (2011).
- Dube, M. G., Horvath, T. L., Leranthe, C., Kalra, P. S. & Kalra, S. P. Naloxone reduces the feeding evoked by intracerebroventricular galanin injection. *Physiol. Behav.* **56**, 811–813 (1994).
- Kalra, S. P. & Horvath, T. L. Neuroendocrine interactions between galanin, opioids, and neuropeptide Y in the control of reproduction and appetite. *Ann. NY Acad. Sci.* **863**, 236–240 (1998).
- Mountjoy, K. G., Mortrud, M. T., Low, M. J., Simerly, R. B. & Cone, R. D. Localization of the melanocortin-4 receptor (MC4-R) in neuroendocrine and autonomic control circuits in the brain. *Mol. Endocrinol.* **8**, 1298–1308 (1994).
- Balthasar, N. *et al.* Divergence of melanocortin pathways in the control of food intake and energy expenditure. *Cell* **123**, 493–505 (2005).
- Leibowitz, S. F. & Hor, L. Endorphinergic and alpha-noradrenergic systems in the paraventricular nucleus: effects on eating behavior. *Peptides* **3**, 421–428 (1982).
- Leibowitz, S. F. Brain neurotransmitters and appetite regulation. *Psychopharmacol. Bull.* **21**, 412–418 (1985).
- Morozov, Y. M. *et al.* Antibodies to cannabinoid type 1 receptor co-react with stomatin-like protein 2 in mouse brain mitochondria. *Eur. J. Neurosci.* **38**, 2341–2348 (2013).
- Morozov, Y. M., Horvath, T. L. & Rakic, P. A tale of two methods: Identifying neuronal CB1 receptors. *Mol. Metabol.* **3**, 338 (2014).
- Bénard, G. *et al.* Mitochondrial CB(1) receptors regulate neuronal energy metabolism. *Nature Neurosci.* **15**, 558–564 (2012).
- Hebert-Chatelain, E. *et al.* Studying mitochondrial CB1 receptors: Yes we can. *Molecular Metabol.* **3**, 339 (2014).
- Hebert-Chatelain, E. *et al.* Cannabinoid control of brain bioenergetics: Exploring the subcellular localization of the CB1 receptor. *Mol. Metabol.* **3**, 495–504 (2014).
- Schneeberger, M. *et al.* Mitofusin 2 in POMC neurons connects ER stress with leptin resistance and energy imbalance. *Cell* **155**, 172–187 (2013).
- Nasrallah, C. M. & Horvath, T. L. Mitochondrial dynamics in the central regulation of metabolism. *Nature Rev. Endocrinol.* **10**, 650–658 (2014).
- Diano, S. *et al.* Peroxisome proliferation-associated control of reactive oxygen species sets melanocortin tone and feeding in diet-induced obesity. *Nature Med.* **17**, 1121–1127 (2011).
- Negre-Salvayre, A. *et al.* A role for uncoupling protein-2 as a regulator of mitochondrial hydrogen peroxide generation. *FASEB J.* **11**, 809–815 (1997).
- Echtay, K. S. *et al.* Superoxide activates mitochondrial uncoupling proteins. *Nature* **415**, 96–99 (2002).
- Andrews, Z. B. *et al.* UCP2 mediates ghrelin's action on NPY/AgRP neurons by lowering free radicals. *Nature* **454**, 846–851 (2008).
- Diano, S. & Horvath, T. L. Mitochondrial uncoupling protein 2 (UCP2) in glucose and lipid metabolism. *Trends Mol. Med.* **18**, 52–58 (2012).
- Huszar, D. *et al.* Targeted disruption of the melanocortin-4 receptor results in obesity in mice. *Cell* **88**, 131–141 (1997).
- Fan, W., Boston, B. A., Kesterson, R. A., Hruby, V. J. & Cone, R. D. Role of melanocortinergic neurons in feeding and the agouti obesity syndrome. *Nature* **385**, 165–168 (1997).
- Cone, R. D. Anatomy and regulation of the central melanocortin system. *Nature Neurosci.* **8**, 571–578 (2005).
- Elias, C. F. *et al.* Leptin differentially regulates NPY and POMC neurons projecting to the lateral hypothalamic area. *Neuron* **23**, 775–786 (1999).
- Cowley, M. A. *et al.* Leptin activates anorexigenic POMC neurons through a neural network in the arcuate nucleus. *Nature* **411**, 480–484 (2001).
- Horvath, T. L., Naftolin, F., Kalra, S. P. & Leranthe, C. Neuropeptide-Y innervation of beta-endorphin-containing cells in the rat mediobasal hypothalamus: a light and electron microscopic double immunostaining analysis. *Endocrinology* **131**, 2461–2467 (1992).
- Soria-Gómez, E. *et al.* The endocannabinoid system controls food intake via olfactory processes. *Nature Neurosci.* **17**, 407–415 (2014).
- Greenberg, I., Kuehnle, J., Mendelson, J. H. & Bernstein, J. G. Effects of marijuana use on body weight and caloric intake in humans. *Psychopharmacology* **49**, 79–84 (1976).
- Foltin, R. W., Brady, J. V. & Fischman, M. W. Behavioral analysis of marijuana effects on food intake in humans. *Pharmacol. Biochem. Behav.* **25**, 577–582 (1986).
- Coppola, A. *et al.* A central thermogenic-like mechanism in feeding regulation: an interplay between arcuate nucleus T3 and UCP2. *Cell Metab.* **5**, 21–33 (2007).
- Parton, L. E. *et al.* Glucose sensing by POMC neurons regulates glucose homeostasis and is impaired in obesity. *Nature* **449**, 228–232 (2007).
- Horvath, T. L. *et al.* Brain uncoupling protein 2: uncoupled neuronal mitochondria predict thermal synapses in homeostatic centers. *J. Neurosci.* **19**, 10417–10427 (1999).
- Andrews, Z. B. *et al.* Ghrelin promotes and protects nigrostriatal dopamine function via a UCP2-dependent mitochondrial mechanism. *J. Neurosci.* **29**, 14057–14065 (2009).
- Landry, M., Vila-Porcile, E., Hokfelt, T. & Calas, A. Differential routing of coexisting neuropeptides in vasopressin neurons. *Eur. J. Neurosci.* **17**, 579–589 (2003).
- van den Pol, A. N. Neuropeptide transmission in brain circuits. *Neuron* **76**, 98–115 (2012).

Supplementary Information is available in the online version of the paper.

Acknowledgements The authors thank M. Shanabrough and J. Bober for technical support and R. Jakab for assisting with the illustrations. This work was supported by the US National Institutes of Health (DP1 DK098058, R01 DK097566, R01 AG040236 and P01 NS062686), the American Diabetes Association, The Klarmann Family Foundation, the Helmholtz Society (ICEMED) and the Deutsche Forschungsgemeinschaft SFB 1052/1 (Obesity Mechanisms).

Author Contributions M.K., S.D. and T.L.H. developed the conceptual framework of this study. M.K., M.O.D., X.-B.G., S.D. and T.L.H. interpreted results. M.K. performed experiments and analysed results. Experimental contributions: L.V. contributed to Figs 4h–j, 5d and Extended Data Figs 1b, 5e and 6a, b; J.G.K. contributed to Figs 2e, f, 3i, 5a, b and Extended Data Fig. 2g; J.D.K. contributed to Figs 3b–d, 5e–g and Extended Data Figs 5c and 6c; F.H. contributed to Figs 4a, 5c and Extended Data Fig. 5a, b, d; S.E.S. contributed to Fig. 3a; C.M.C., C.R.V. and J.K.E. provided key animal models; Y.M.M. and P.R. contributed to Fig. 3b and Extended Data Fig. 1c; P.R., I.B. and M.A.C. provided materials, animals and equipment; K.S.-B. contributed to Figs 3f and 4d–g; X.-B.G. contributed to Figs 1C, D–c and 3j. M.K. and T.L.H. wrote the paper.

Author Information Reprints and permissions information is available at www.nature.com/reprints. The authors declare no competing financial interests. Readers are welcome to comment on the online version of the paper. Correspondence and requests for materials should be addressed to T.L.H. (tamas.horvath@yale.edu).

METHODS

All used mice were aged between 10 and 18 weeks at the time of killing. All procedures were approved by Yale University Institutional Animal Care and Use Committee (IACUC). Mice were maintained under standard laboratory conditions with water and food freely available unless otherwise stated. Mice were housed on a 12 h light/12 h dark cycle with lights on at 07:00 and off at 19:00. All experimental groups within one experiment contained mice of same strain and sex, being similar in age and body weight, showing no difference in physical activity and feeding behaviour when assessed before drug injections. Starting at 13–14 weeks of age, body weights differed between wild-type and *Cnr1*^{-/-} littermates. Animals from different experimental groups (vehicle versus drug treatment) were randomly allocated within the experimental order. After finishing experiments (data collection), each mouse ID was modified by a second investigator to blind the respective investigator who performed data analyses.

Mice. *Pomc topaz* (*Pomc-GFP*) transgenic mice were provided by J. Friedman and generated as described earlier⁴⁸. The *Npy-hrGFP* line (strain B6.FVB-Tg(*Npy-hrGFP*)1Lowl/J) and *Pomc-Cre* line (strain Tg(*Pomc1-cre*)16Lowl/J) were purchased from The Jackson Laboratories. *Pomc-GFP* and *Npy-hrGFP* lines are maintained on a C57BL6 background; the *Pomc-Cre* line is maintained on a mixed background in our laboratory. Note that *Npy-hrGFP* mice allow visualization of AgRP neurons through co-expression of NPY and AgRP in these cells. The first CB₁R knockout (*Cnr1*^{-/-}) line used here, as maintained in a C57BL6 background, was generated (sponsored by NIMH) and genotyped as previously described⁴⁹. This line was used for feeding studies (Extended Data Fig. 1c) and ELISA experiments (Fig. 3b). For generation of the second *Cnr1*^{-/-} line used here, mice bearing the transcription blocking cassette flanked by *loxP* sites upstream of the *Cnr1* start codon (*Cnr1*+/TB-*lox*) were crossed with transgenic mice expressing *Pomc-Cre*. Offspring expressing *Cnr1*TB/+, *Pomc-Cre* were mated with *Cnr1*TB/+ to obtain littermate controls (wild-type; *Pomc-Cre*::*Cnr1*+/+ and *Cnr1*+/+), CB₁R knockout controls (TB-CB₁R; *Cnr1*TB/TB), and mice expressing CB₁R only in POMC neurons (CB₁RPOMC; *Pomc-Cre*::*Cnr1*TB/TB). These mice were used for specification of POMC CB₁R expression and for validation of CB₁R antibody specificity (Extended Data Fig. 5e). The original breeding pairs of the UCP2 knockout (*Ucp2*^{-/-}) line were provided by B. Lowell and were generated as reported previously⁵⁰. C57BL6 mice were purchased from The Jackson Laboratories.

Chemicals and antibodies. The selective CB₁R agonist arachidonoyl 2-chloroethylamide (ACEA; Tocris Biosciences) was delivered pre-dissolved in ethanol (5 mg ml⁻¹). For central injection of ACEA, ethanol was evaporated and ACEA was re-dissolved in dimethylsulfoxide (DMSO). The CB₁R agonist WIN-55,212-2 mesylate (WIN) and the CB₁R inverse agonist rimobant (RIMO; Cayman Chemical Company) were dissolved in DMSO and aliquots were stored as a stock solution of 10 mg ml⁻¹ at -80 °C for 3 months or less. At the day of use, ACEA, WIN or RIMO was mixed with a small drop of Tween 80 (Sigma-Aldrich) before further dilution in saline and applied intraperitoneally to the animals. For the vehicle group, the same volume of ethanol or DMSO was applied compared to ACEA, WIN or RIMO. Clozapine-*N*-oxide (CNO; Enzo Life Sciences) was dissolved in saline (5 mg ml⁻¹) and stored at -80 °C until day of use. The μ -opioid receptor antagonist naloxone (naloxone hydrochloride; Tocris Bioscience) was dissolved in saline (100 mg ml⁻¹) and stored at -80 °C until day of use. Dihydroethidium (DHE; 10 \times 1 mg; Life Technologies) was stored light protected at -20 °C until use. Hoechst 33342 trihydrochloride, trihydrate (100 mg; Invitrogen) was stored light protected at 4 °C. Virus molecules (4 \times 10¹² per ml, dialysed in 350 mM NaCl plus 5% D-sorbitol in PBS) containing inhibitory DREADD (rAAV5/EF1 α -DIO-hM4D(Gi)-mCherry) or stimulating DREADD (rAAV5/EF1 α -DIO-hM3D(Gq)-mCherry) were purchased from Gene Therapy Center Vector Core. Aliquots were stored at -80 °C. The used primary and corresponding secondary antibodies were stored according to manufacturer's instructions. Primary antibodies are summarized in Supplementary Table 1.

Immunofluorescence. After removal of food at 10:00, fed male mice were injected intraperitoneally with vehicle, WIN (1 mg kg⁻¹ body weight) or ACEA (1 or 5 mg kg⁻¹) for 90 min. Overnight fasted male mice were injected (intraperitoneally) with vehicle or RIMO (3 mg kg⁻¹) at 10:00 for 90 min. Mice were then anaesthetized by isoflurane and killed by perfusion fixation (4% paraformaldehyde (PFA) in 0.1 M PBS), followed by overnight post-fixation in 4% PFA. After 30 min washing in PBS, brains were cut into 50- μ m-thick sections, and 12 sections per mouse containing the ARC were collected. After 15 min in PBS, the sections were incubated in blocking solution (1:20 normal donkey serum in PBS (in case of CB₁R staining using antisera derived from guinea-pig, 1:20 normal goat serum was used), containing 0.2% Triton X-100) for 30 min at room temperature. Primary antibodies (see Supplementary Table 1) were then applied overnight at room temperature. The next day, sections were washed three times (5 min) in PBS and incubated with the respective secondary antibodies for 1 h at room

temperature (donkey anti-rabbit IgG fluor 488 or 568 (dilution 1:250, A-11008; or dilution 1:750, A-11036); donkey anti-sheep IgG fluor 488 (dilution 1:250, A-11015); goat anti-guinea-pig IgG fluor 488, 568 or 633 (dilution 1:250; A-11073; dilution 1:750, A-11075; or dilution 1:500, A-21105); goat anti-mouse fluor 633 (dilution 1:500; A-21052); Life Technologies). Finally, the sections were cover-slipped. Double immunofluorescence labelling for cFOS and POMC in *Pomc-Cre* mice started with incubation of sections in blocking solution (see above). The anti-cFOS antibody was incubated at room temperature overnight. The next day, sections were incubated in biotinylated goat anti-rabbit IgG (dilution 1:250; BA-1000, Vector Laboratories) for 2 h at room temperature. After washing in PBS, sections were incubated in avidin, conjugated with Alexa Fluor 488 (dilution 1:2,500, A-21370, Life Technologies) for 1 h at room temperature. After washing in PBS, sections were incubated in unconjugated anti-rabbit IgG (dilution 1:25; 711-005-152, Jackson ImmunoResearch Laboratories) for 2 h at room temperature. After washing in PBS, the sections were incubated with anti-POMC antibody overnight at room temperature. Finally, sections were incubated with goat anti-rabbit Alexa Fluor 633 (dilution 1:750, A-21070, Life Technologies) in PBS for 1 h at room temperature. Confocal laserscanning microscopy was performed using a Zeiss LSM510 Meta, the confocal system equipped with helium neon lasers (543 and 633 nm excitation lines) and an argon laser (488 nm). Quantification of cFOS and pCREB immunoreactivity in *Pomc-GFP* and *Pomc-Cre* mice was performed by counting the percentage of cFOS- and pCREB-positive POMC-GFP or POMC-immunolabelled cells in 10- μ m optical, confocal sections obtained from 50- μ m-thick vibratome sections. For each mouse, at least 3–4 50- μ m-thick sections containing the ARC were analysed.

Immunocytochemistry for electron microscopy. Male C57BL6 mice were anaesthetized and transcardially perfused with 4% PFA and 0.1% glutaraldehyde. After post-fixation overnight, vibratome sections (50 μ m) containing the ARC were immunostained. After overnight incubation of primary antibodies (see Supplementary Table 1), sections were washed, incubated with biotin-conjugated donkey anti-rabbit IgG secondary antibody (dilution 1:250, 711-065-152, Jackson ImmunoResearch Laboratories) for 2 h, washed again, put in avidin-biotin complex (ABC; Vector Laboratories), and developed with 3,3'-diaminobenzidine (DAB). After washing, sections were incubated in 6 nm colloidal gold-conjugated donkey anti-sheep IgG secondary antibody (dilution 1:50, 713-195-147, Jackson ImmunoResearch Laboratories) for 2 h. Sections were then osmicated (15 min in 1% osmium tetroxide) and dehydrated in increasing ethanol concentrations. During the dehydration, 1% uranyl acetate was added to the 70% ethanol to enhance ultrastructural membrane contrast. Flat embedding in Durcupan followed dehydration. Ultrathin sections were cut on a Leica ultra microtome, collected on Formvar-coated single-slot grids, and analysed with a Tecnai 12 Biotwin electron microscope (FEI).

Semi-quantitative measurements of α -MSH and β -endorphin immunostaining. Analyses of α -MSH and β -endorphin immunosignals in male mice were performed by use of ImageJ 1.48 s software, following the online tutorial for area measurements and particle counting (<http://imagej.nih.gov/ij/docs/pdfs/examples.pdf>). In brief, confocal stack images (*z*-stacks; thickness/optical section: 6 μ m, resolution: 1,024 \times 1,024 pixels) of one side of the PVN were obtained from 50- μ m-thick vibratome brain sections, using the same magnification and the same confocal microscope setup for all samples. All images from the different experimental groups in one experiment were taken within the same session at the confocal microscope (Zeiss LSM510 Meta). For *z*-projection, five optical sections from the middle area of each brain slice were used. Images were converted into greyscale (8 bit) and binary images were created. For particle analysis, the range of particle size (in pixel units) was set to resemble α -MSH and β -endorphin immunosignals in the PVN and to avoid selection of unspecific background staining. The same range of particle size was used for all samples. Finally, total numbers of selections ('number'), the sum of the size of all selections ('area'; in square pixels) and the sum of the average grey values of all selection ('mean' grey values) were calculated.

Electrophysiology. Coronal hypothalamic slices containing the ARC of male *Pomc-gfp* or *NPY-hrGFP* mice (3–4 weeks old) were prepared 90 min after *in vivo* saline or ACEA (1 mg kg⁻¹ body weight) treatment, as described previously⁵¹. In brief, mice were anaesthetized with isoflurane and decapitated, the brain was rapidly removed and immersed in a cold (4 °C) and oxygenated cutting solution containing (mM): sucrose 220, KCl 2.5, NaH₂PO₄ 1.23, NaHCO₃ 26, CaCl₂ 1, MgCl₂ 6 and glucose 10 (pH 7.3 with NaOH). Coronal hypothalamic slices (300 μ m thick) were cut with a Leica vibratome after the brain was trimmed to a small tissue block containing the hypothalamus. After preparation, slices were maintained at room temperature (23–25 °C) in a storage chamber in the aCSF (bubbled with 5% CO₂ and 95% O₂) containing (in mM): NaCl 124, KCl 3, CaCl₂ 2, MgCl₂ 2, NaH₂PO₄ 1.23, NaHCO₃ 26, glucose 10 (pH 7.4 with NaOH) for recovery and storage. After recovery at room temperature for at least 1 h, slices were transferred to a recording chamber constantly perfused with bath solution (same as the aCSF except

containing 2.5 mM glucose) at a temperature of 33 °C and a perfusion rate of 2 ml min⁻¹ for electrophysiological experiments. Whole-cell patch-clamp recording was performed in *Pomc-GFP* and *Npy-hrGFP* neurons under current clamp with the methods previously reported⁵¹. Spontaneous membrane and action potential was recorded for 10 min in *Pomc-GFP* and *Npy-hrGFP* neurons from both control and ACEA-treated mice.

To test the effects of ACEA on POMC neurons *in vitro*, hypothalamic slices containing the ARC were prepared from naive male *Pomc-GFP* mice. After a stable recording of membrane and action potential under current clamp or membrane current under voltage clamp (at -60 mV), ACEA was applied, in the presence or absence of TTX (0.5 μM), to the recorded cells through bath application for 10 min. The micropipettes (4–6 MΩ) were made of borosilicate glass (World Precision Instruments) with a micropipette puller (Sutter P-97) and back filled with a pipette solution containing (mM): K-gluconate 135, MgCl₂ 2, HEPES 10, EGTA 1.1, Mg-ATP 2.5, Na₂-GTP 0.3, and Na₂-phosphocreatin 10 (pH 7.3 with KOH). Both input resistance and series resistance were monitored throughout the experiments and the former was partially compensated. Only recordings with stable series resistance and input resistance were accepted. All data were sampled at 3–10 kHz, filtered at 3 kHz and analysed with an Apple Macintosh computer using AxoGraph X (Kagi).

Behavioural test (open field). A slightly modified experimental regimen according ref. 52 was used. The apparatus consists of a Plexiglas open field (37 × 37 × 37 cm). Male C57BL6 mice habituated for single cage housing and intraperitoneal injection (see 'food intake measurements'), were put in the open field for 90 min after injection with vehicle or ACEA (5 mg kg⁻¹ body weight) and locomotor activity was monitored.

Central cannula placement. Anaesthetized (in mg kg⁻¹ body weight: intraperitoneal, 30 ketamine, 6 xylazine; subcutaneous; 0.1 buprenorphine) 10-week-old male C57BL6 or 12-week-old male *Pomc-gfp* mice were placed into a stereotaxic apparatus (model 902; David Kopf instruments). The head was cleaned with alcohol pads and incision was made with a sterile scalpel. To place the guide acute cannula (C315GA/SPC, 26 gauge, 8 mm pedestal size, 6.5 mm below pedestal; Plastics One), a single hole was drilled according to the following coordinates: ARC, bregma, anterior–posterior: -1.2 mm, lateral: +0.25 mm; PVN, bregma, anterior–posterior: -0.6 mm, lateral: +0.25 mm). The guided cannula was placed 1 mm dorsal to the region of interest to minimize damage of target area (ARC, bregma, dorsal–ventral: -5.0 mm, PVN, dorsal–ventral: -4.5 mm). The cannula was fixed in place with acrylic dental cement and one anchoring skull screw. After 30 min, a dummy cannula (C315DC/SPCA, cut length, 1 mm extension) was twisted onto the guided cannula. Mice were allowed to recover for 1 week, monitoring food intake and body weight. Mice with abnormal food intake or body weight were excluded. Mice were handled daily and habituated to the injection procedure for 5 days before experimental procedures. At the day of experiment, mice were held gently, while the dummy cannula was removed and the internal cannula (C315IA/SPC, 33 gauge, 8 mm pedestal size, cut length, 1 mm extension) was inserted. The internal cannula was connected to a plastic tube containing a Hamilton syringe at its end, allowing free movement of mice during injection. For PVN, NALO (5 μg per 0.5 μl saline, injection time 1 min) was injected 5 min before peripheral (intraperitoneal) injection of ACEA or WIN. For ARC, ACEA (1 μg per 0.5 μl saline (10% DMSO, 0.2% Tween-80); 1 min) was added. RIMO (1.25 μg per 0.5 μl saline (25% DMSO, 0.2% Tween-80); 1 min) was injected 5 min before peripheral (intraperitoneal) injection of ACEA or WIN. Internal cannula was kept in brain for another minute before replacement and, finally, dummy cannula was twisted onto guided cannulas and food intake was monitored for 1 and 2 h. In previous experiments equal volume injection of the fluorescent dye Hoechst 33342 (1:10 in saline) into the PVN or ARC was identified as an ideal spread of injection. After finishing food intake experiments, Hoechst 33342 was also used to assess correct cannula placement. Mice with missed target areas were excluded.

Stereotaxic virus injection. Animals were injected as described earlier^{5,53}. In brief, bilateral virus injections were made into the ARC of anaesthetized (see 'central cannula placement') 12-week-old male *Pomc-Cre* mice, placed into a stereotaxic apparatus (model 902; David Kopf instruments). Viruses (200 nl) containing the inhibitory DREADD (rAAV5/EF1α-DIO-hM4Di-mCherry) or the stimulating DREADD (rAAV5/EF1α-DIO-hM3Dq-mCherry) were applied into each hemisphere (coordinates: bregma, anterior–posterior: -1.2 mm, dorsal–ventral: -5.8 mm, lateral: ±0.3 mm) by using an air pressure system (injection time 5 min). After surgery, mice were allowed to recover for 1 week and were then acclimated for food intake experiments (see 'food intake measurements'). After finishing the feeding experiments, mice were transcardially perfused and 50-μm-thick vibratome sections of the ARC were prepared. Accurate virus injection into the ARC was verified by analysing local mCherry fluorescence. Mice with 'missed' or 'partial' hits were excluded. Specific (virus) expression in ARC POMC neurons was signified by double fluorescence labelling for mCherry and POMC (see 'immunofluorescence').

Food intake measurements. One week before starting experiments, animals were allowed to habituate to single cage housing. Sham injections were performed 2 days before starting the experiment. The day before experiment, single home cages were changed to avoid mice eating food that may have been deposited in the bedding of the cages. To generally minimize disposal of food, the animals were adapted to lower amounts of food (15–25 g per cage) at starting adaption to single housing. To analyse the effect of the CB₁R agonist ACEA or the CB₁R agonist WIN on food intake in fed animals, food was removed, new pre-weighed food pellets were applied and food intake of each single-housed animal was measured 1, 2 and 24 h after intraperitoneal injection of ACEA or WIN, compared to vehicle, respectively (injection time: 09:00). In the DREADD feeding experiments, CNO (0.3 mg kg⁻¹ body weight; intraperitoneal) was injected 15 min before cannabinoid (ACEA or WIN) treatment. To investigate whether cannabinoid (ACEA or WIN)-induced feeding is mediated via β-endorphin release, the μ-opioid receptor antagonist naloxone (7.5 mg kg⁻¹ body weight; intraperitoneal) was injected 15 min before cannabinoid (ACEA or WIN) administration and food intake was analysed 1 h after injection. To address the question whether CB₁R inverse agonist RIMO reduced fasting-induced re-feeding, the single-housed animals were fasted overnight before intraperitoneal injection of 3 mg kg⁻¹ RIMO or vehicle (injection time: 09:00). Fifteen minutes after RIMO injection, a pre-weighed amount of food was placed into the cage and the food intake was then calculated for 1, 2 and 24 h. At all times the cages were inspected for food spillage and those mice in cages with visible food deposits in the bedding were excluded from the studies.

Radioimmunoassay. Male C57BL6 mice were killed by decapitation and brains were immediately removed. A block of the hypothalamus was cut and a 2-mm slice of the mediobasal forebrain was made using a Leica VT1000P vibratome. Each slice was first incubated with aCSF in an incubator (37 °C, 95% O₂ and 5% CO₂) for 1 h. This was followed by another incubation in aCSF, followed by incubation in aCSF (control) or in aCSF containing 100 nM ACEA (both groups containing 56 mM KCl) for 45 min. The supernatant was then removed and frozen for future RIA analysis. The α-MSH and β-endorphin radioimmunoassays were performed following instructions of the Phoenix pharmaceutical RIA kit (α-MSH, RK-043-01; β-endorphin, RK-022-33).

ELISA. *Ex vivo* measurements of β-endorphin content in mediobasal hypothalamus derived from male wild-type and corresponding *Cnr1*^{-/-} littermates was assessed by use of a commercially available β-endorphin ELISA kit and in accordance to manufacturer's instructions (MyBioSource, MBS703919). In brief, 30 mg of tissue was rinsed and mechanically homogenized in PBS. After two freeze-thaw cycles, the homogenates were centrifuged for 5 min at 5,000g and 4 °C. The supernatant was removed and assayed immediately. In parallel, sample protein concentrations were measured using the BCA kit (Thermo scientific, 23228 and 1859078), and β-endorphin content was calculated as nanograms β-endorphin per milligram protein.

qPCR and western blot analyses. Food was removed from cages of fed mice. Male C57BL6 mice were then treated with vehicle or ACEA (1 mg kg⁻¹ body weight, intraperitoneal) as described above. After 90 min, the mediobasal hypothalamus was rapidly collected and snap frozen in liquid nitrogen. Total RNA was extracted using TRIzol (Life Technologies) according to manufacturer's instructions. cDNA was synthesized by First-Strand cDNA Kit (Amersham Biosciences) following the manufacturer's instructions. Real-time PCR (Light Cycler 480 System, Roche) was performed using TaqMan gene expression assay for *Psc1*, *Psc2*, *Ucp2* and *Cnr1* (Mm00479023_m1, 4331182; Mm00500981_m1, 4331182; Mm00627599_m1, 4331182; Mm01212171_s1, 4331182; Life Technologies). β-actin (mouse *Actb*, 4352341; Life Technologies) was used as housekeeping gene.

Micro-punched ARC from fed male C57BL6 mice, either treated with vehicle or ACEA (1 mg kg⁻¹ body weight, intraperitoneal) for 90 min after removal of food, were isolated and lysed in modified RIPA buffer (50 mM Tris-HCl, pH 7.5; 150 mM NaCl, 1 mM EDTA, 1% NP-40, 0.1% SDS, 1 mM PMSF), supplemented with protease inhibitor cocktail (Roche, 11 836 170 001), on ice for 30 min followed by centrifugation at 14,000 r.p.m. for 15 min. Protein concentrations were measured using the BCA kit (Thermo Scientific). Proteins were resolved on 8% SDS-PAGE and transferred to PVDF membrane (Millipore, IPVH 15150). Membranes were blocked with 5% dry milk in TBS (50 mM Tris-HCl, pH 7.5; 150 mM NaCl) for 1 h and then followed by overnight incubation at 4 °C with first antibodies (see Supplementary Table 1). After three washes with TBST (TBS plus 0.05% Tween 20), membranes were incubated with anti-rabbit IgG conjugated to horseradish peroxidase (Santa Cruz Biotechnology, sc-2004) for 1 h and developed by ECL kit (Thermo Scientific, 32016). Membranes were reused to detect β-actin (see Supplementary Table 1) after stripping with Restore PLUS Western Blot stripping buffer (46430, Thermo Fisher Scientific). The relative protein amount of PC-1, PC-2 and POMC in each sample was calculated from the respective β-actin immunosignal. **ROS measurement.** After removal of food at 10:00, fed age- and weight-matched littermates of male and female *Pomc-GFP* mice were injected with vehicle or

1 mg kg⁻¹ ACEA (intraperitoneal) for 90 min. DHE (10 mg) was dissolved in 200 µl DMSO 5 min before injection and kept light-protected at room temperature. Then 240 µl of warm (42 °C) PBS was slowly mixed with 60 µl DHE solution, and 200 µl of the DHE solution (1 mg ml⁻¹ in 20% DMSO) was injected via the tail vein 45 min before the animals were anaesthetized by isoflurane and killed by perfusion fixation (4% PFA in 0.1 M PBS). After post-fixation in 4% PFA overnight, the brains were washed in PBS for 30 min and coronal brain sections (50 µm) of the ARC were obtained using a Leica VT1000P vibratome (Leica Microsystems). The slices were mounted on glass slides and coverslipped using DAKO fluorescence mounting medium (Dako North America) and kept at 4 °C for no longer than 1 day. Confocal images were taken by use of an Olympus FV 300 Laserscanning microscope. Semi-quantitative analysis of the DHE signal in *Pomc-GFP* labelled cells was performed by determine the mean dens area of the DHE signal in the respective GFP positive neuron, using imagej 1.48 s software (Rasband, W.S., ImageJ, US National Institutes of Health). To avoid false-positive results, the autofluorescence in animals that were injected with saline instead of DHE was subtracted from the DHE-obtained values.

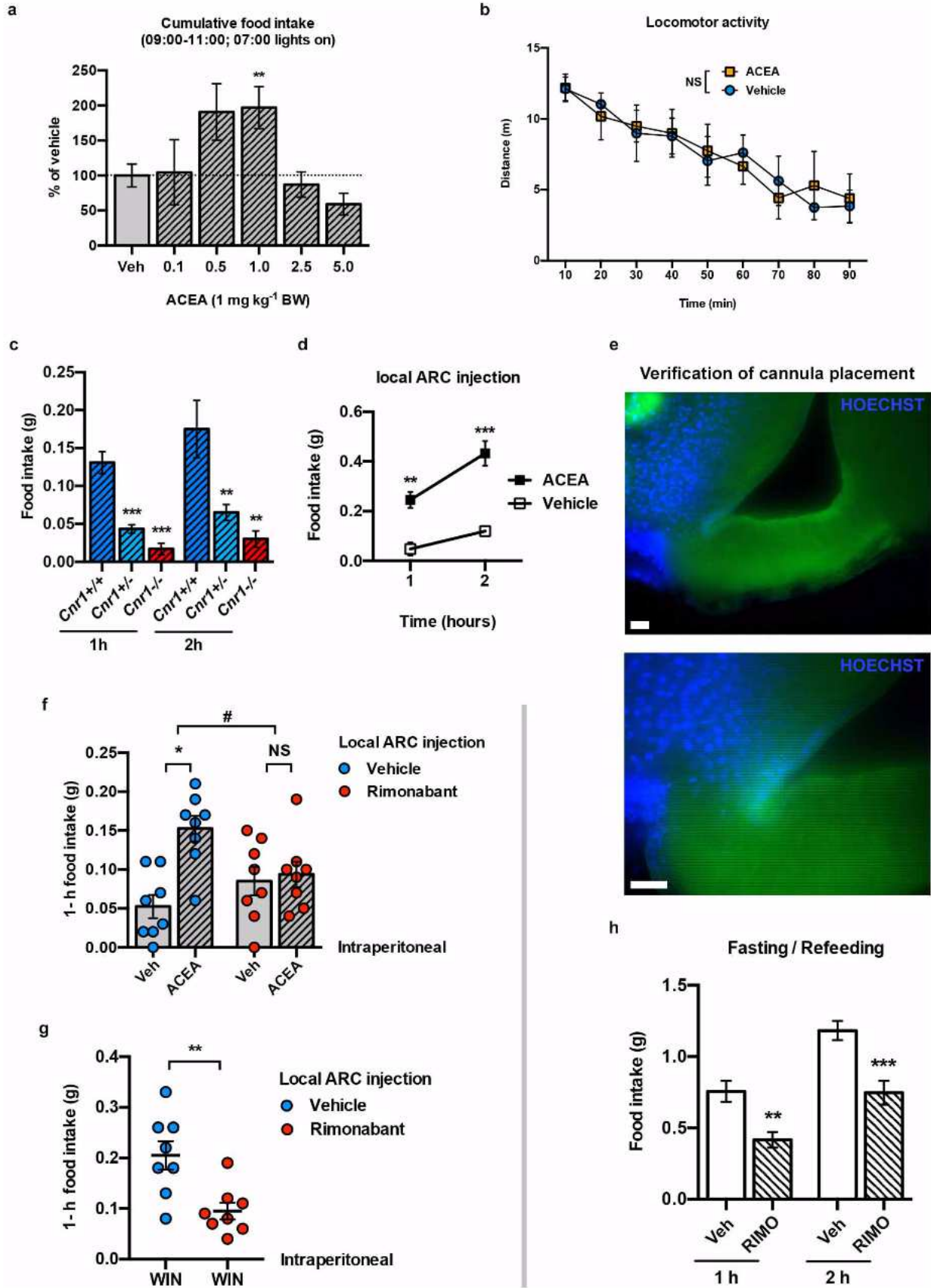
Brain tissue fractionation. Mouse brain homogenates were purified using a differential centrifugation method described earlier⁵⁴. After removal of food from cages, mice were injected with vehicle or ACEA for 90 min. For isolation of mitochondria-enriched fractions, male and female C57BL6, *Ucp2*^{-/-} and corresponding wild-type littermates were killed and both the hippocampus and the hypothalamus were immediately dissected from brains and put on ice. Tissue was manually homogenized at 4 °C in 10 ml of isolation buffer containing 225 mM mannitol, 75 mM sucrose, 5 mM HEPES, 1 mM EGTA, 1 mg ml⁻¹ BSA and 0.3125 mg ml⁻¹ protease type VIII (Sigma-Aldrich) at pH 7.4. The homogenate was brought to 20 ml final volume and centrifuged at 2,000g for 5 min. The pellet, including the synaptosomal layer was re-suspended in 10 ml of the isolation buffer now containing 0.02% (w/v) digitonin and centrifuged at 12,000g for 10 min. The pellet without the synaptosomal layer was re-suspended in 10 ml of isolation buffer and centrifuged at 12,000g for 10 min. The pellet was finally re-suspended in 50 µl of a buffer containing 225 mM mannitol, 75 mM sucrose, 5 mM HEPES at pH 7.4.

Ex vivo mitochondrial respiration. Protein concentrations of mitochondrial preparations were determined with a BCA protein assay kit (Perbio). For mitochondrial respiration analyses, 0.5 mg ml⁻¹ protein was added into the reaction

chamber of a Clark type oxygen electrode (Hansatech Instruments) which has been set to 37 °C and filled with 1 ml respiration buffer (100 mM sucrose, 5 mM HEPES, 100 mM KCl, 2 mM KH₂PO₄ and 10 µM EGTA, pH 7.4). Pyruvate (5 mM) and malate (2.5 mM) were then added concomitantly as the oxidative substrates. To determine ADP-dependent (state 3) respiration, ADP (2.5 mM) was added. After the ADP was exhausted, oligomycin (1 µM) was applied to analyse respiration independently of phosphorylation (state 4 activity).

Statistics. Statistical analyses were performed by use of Prism 6.0 software (Graph Pad). *P* < 0.05 was considered statistically significant. *P* values for unpaired comparisons between two groups were calculated by two-tailed Student's *t*-test. One-way ANOVA, followed by Dunnett's multiple comparisons test (all groups against vehicle-treated control group) was used for comparisons between three or more groups. Ordinary two-way ANOVA, followed by Sidák's multiple comparison test was used to examine how food intake was affected by two factors. Interactions between the following treatments were tested: CNO against ACEA or WIN; RIMO against ACEA or WIN; NALO against ACEA or WIN; ACEA treatment against genotype (wild-type littermates versus *Ucp2*^{-/-} mice). **P* < 0.05, ***P* < 0.01, ****P* < 0.001. Error bars indicate mean ± s.e.m. No statistical methods were used to predetermine sample size.

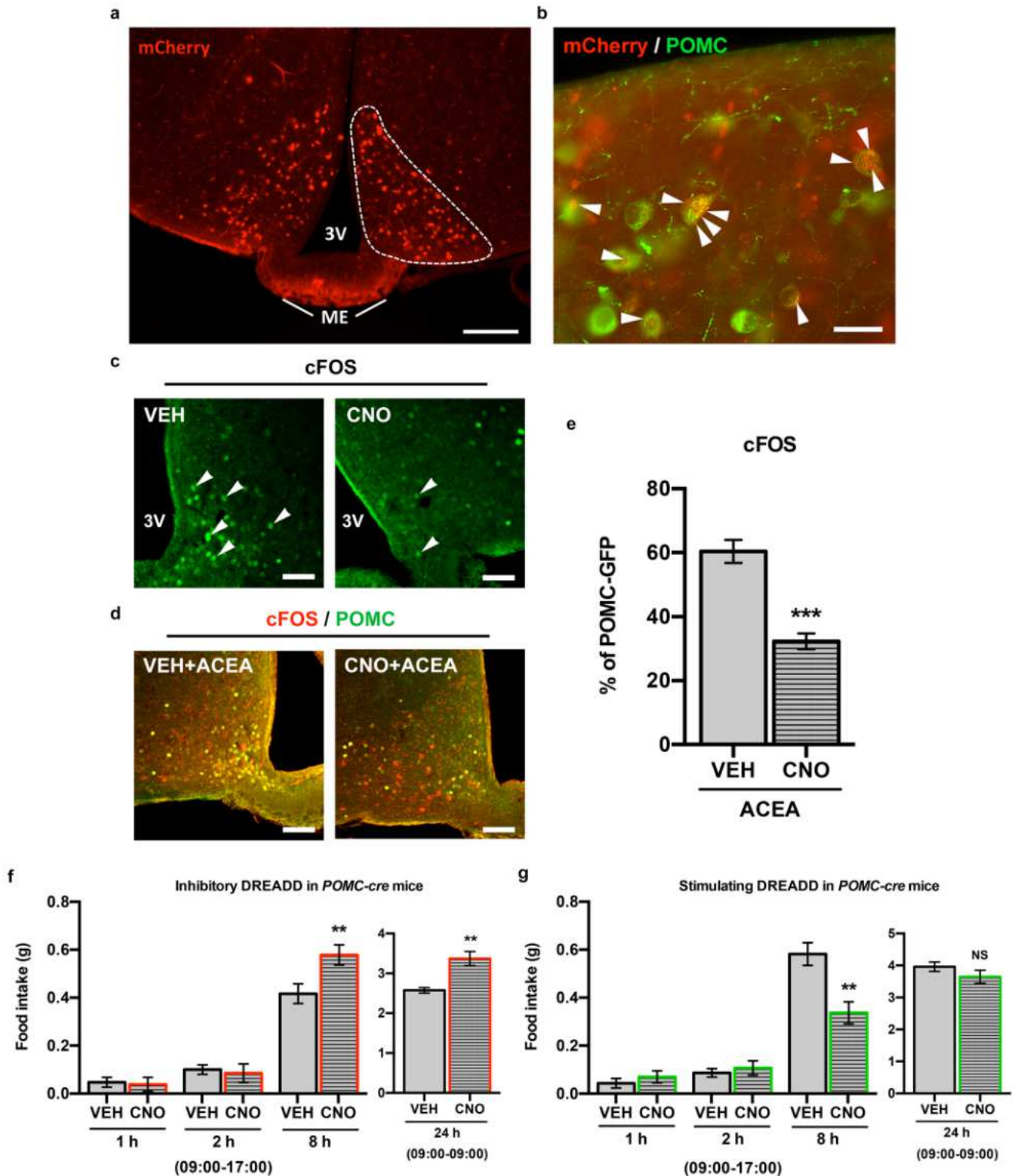
48. Pinto, S. *et al.* Rapid rewiring of arcuate nucleus feeding circuits by leptin. *Science* **304**, 110–115 (2004).
49. Zimmer, A., Zimmer, A. M., Hohmann, A. G., Herkenham, M. & Bonner, T. I. Increased mortality, hypoactivity, and hypoalgesia in cannabinoid CB1 receptor knockout mice. *Proc. Natl Acad. Sci. USA* **96**, 5780–5785 (1999).
50. Zhang, C. Y. *et al.* Uncoupling protein-2 negatively regulates insulin secretion and is a major link between obesity, beta cell dysfunction, and type 2 diabetes. *Cell* **105**, 745–755 (2001).
51. Dietrich, M. O., Liu, Z. W. & Horvath, T. L. Mitochondrial dynamics controlled by mitofusins regulate *AgRP* neuronal activity and diet-induced obesity. *Cell* **155**, 188–199 (2013).
52. Dietrich, M. O. *et al.* *AgRP* neurons regulate development of dopamine neuronal plasticity and nonfood-associated behaviors. *Nature Neurosci.* **15**, 1108–1110 (2012).
53. Cetin, A., Komai, S., Eliava, M., Seeburg, P. H. & Osten, P. Stereotaxic gene delivery in the rodent brain. *Nature Protocols* **1**, 3166–3173 (2006).
54. Moreira, P. I. *et al.* Mitochondria from distinct tissues are differently affected by 17β-estradiol and tamoxifen. *J. Steroid Biochem. Mol. Biol.* **123**, 8–16 (2011).



Extended Data Figure 1 | Characterization of CB₁R-dependent food intake.

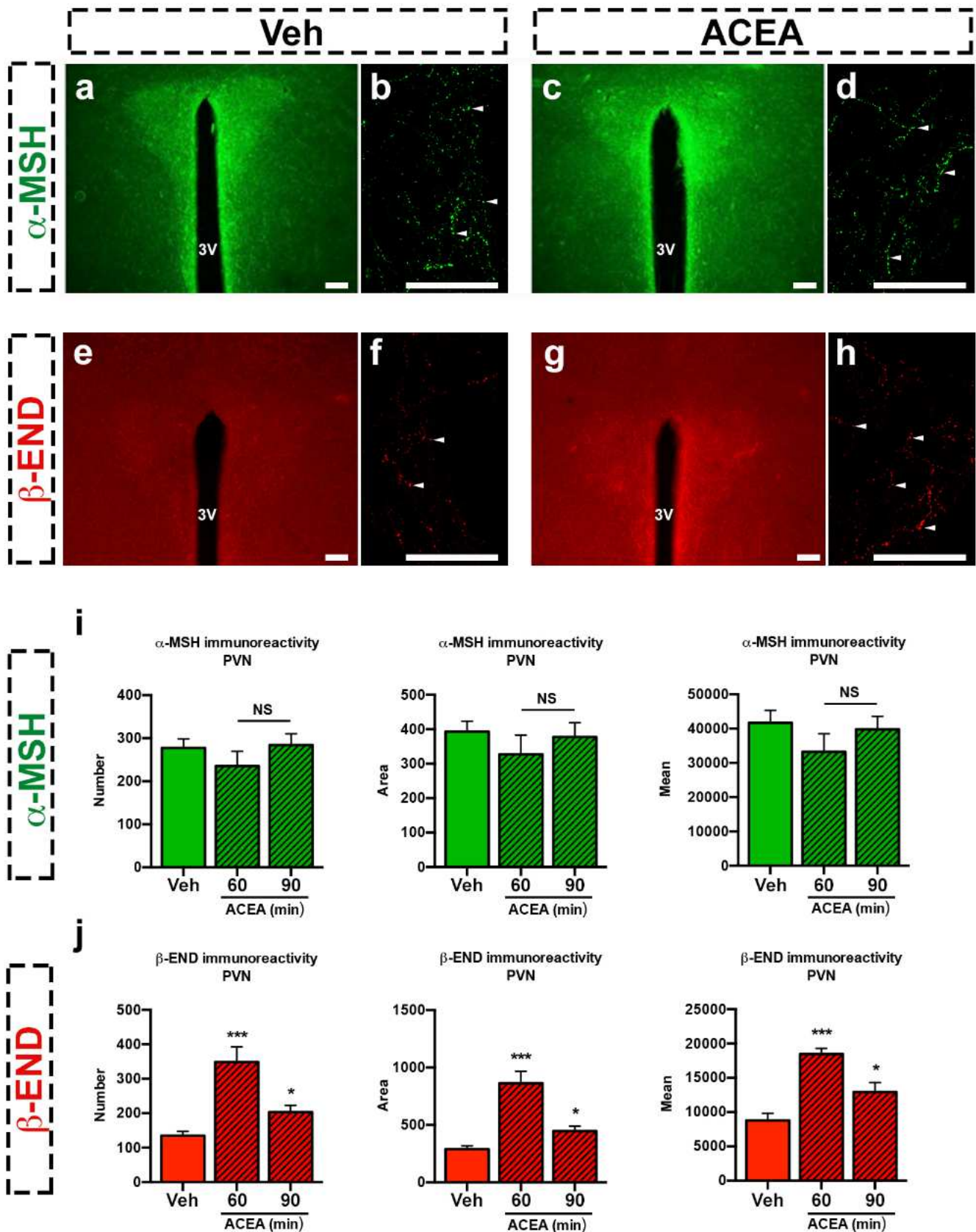
a, Bimodal effects of different ACEA doses on food intake in fed mice (vehicle, $n = 23$ mice, $100 \pm 16.3\%$; ACEA (in mg kg^{-1} body weight, intraperitoneal): 0.1, $n = 8$, $104.5 \pm 46.6\%$; 0.5, $n = 3$, $190.8 \pm 40.4\%$; 1.0, $n = 19$, $196.7 \pm 30\%$; 2.5, $n = 16$, $87.1 \pm 18\%$; 5.0, $n = 11$, $59.2 \pm 15.5\%$; $**P < 0.01$ versus vehicle, one-way ANOVA, followed by Dunnett's multiple comparisons test; six independent experiments with litters from different parents). **b**, Neutral dose of ACEA on feeding (5 mg kg^{-1} body weight, intraperitoneal) did not alter locomotor activity of fed mice ($n = 3$ mice/group; $P > 0.05$). **c**, Impaired feeding response to ACEA (1 mg kg^{-1} body weight, intraperitoneal) in CB₁R-heterozygote mice ($Cnr1^{+/-}$, $n = 6$ mice, 1 h: 0.04 ± 0.01 g, 2 h: 0.07 ± 0.01 g) and CB₁R-deficient mice ($Cnr1^{-/-}$, 1 h: $n = 6$, 0.02 ± 0.01 g, 2 h: $n = 4$, 0.03 ± 0.01 g) mice, when compared to CB₁R wild-type mice ($Cnr1^{+/+}$, 1 h: $n = 12$, 0.13 ± 0.01 g, 2 h: $n = 4$, 0.18 ± 0.04 g; $**P < 0.01$, $***P < 0.001$ versus wild-type; two independent experiments). **d**, Central, local ACEA injection into the ARC induced food intake (vehicle, $n = 4$ mice, 1 h: 0.05 ± 0.03 g, 2 h: 0.12 ± 0.01 g; ACEA, $n = 4$, 1 h: 0.25 ± 0.03 g; 2 h: 0.43 ± 0.05 g; $**P < 0.01$, $***P < 0.001$). **e**, Verification of correct ARC cannula placement by

HOECHST (blue) injection (representative image (two different magnifications) of four independent experiments). **f**, Hyperphagic CB₁R activation (1 mg kg^{-1} body weight ACEA, intraperitoneal) was abolished by central, local ARC RIMO-mediated CB₁R blockade (vehicle plus vehicle, $n = 8$ mice, 0.05 ± 0.01 g; vehicle plus ACEA, $n = 8$, 0.15 ± 0.02 g; RIMO plus vehicle, $n = 8$, 0.09 ± 0.02 g; RIMO plus ACEA, $n = 8$, 0.09 ± 0.02 g; $*P < 0.05$, $\#P < 0.05$ for interaction between RIMO and ACEA, two-way ANOVA, followed by Šidák's multiple comparisons test; two independent experiments). **g**, Hyperphagic CB₁R activation (1 mg kg^{-1} body weight WIN, intraperitoneal) was reduced by local ARC RIMO-mediated CB₁R blockade (vehicle plus WIN, $n = 8$ mice, 0.21 ± 0.03 g; RIMO+WIN, $n = 8$, 0.1 ± 0.02 g; $***P < 0.01$). **h**, RIMO-induced hypophagic blockade of CB₁R in fasted mice (vehicle, $n = 10$ mice, 1 h: 0.76 ± 0.07 g, 2 h: 1.18 ± 0.07 g; RIMO, $n = 11$ mice, 1 h: 0.42 ± 0.05 g, 2 h: 0.75 ± 0.08 g; $**P < 0.01$, $***P < 0.001$; two independent experiments). Values (biological replicates) denote mean \pm s.e.m. If not otherwise stated, P values (unpaired comparisons) by two-tailed Student's t -test. Scale bars, $25 \mu\text{m}$.



Extended Data Figure 2 | DREADD-mediated regulation of POMC neurons. **a**, Selective DREADD expression specified by local ARC mCherry fluorescence. **b**, POMC neurons (green) contain mCherry-labelled DREADD (red, arrowheads). **c**, CNO-activated inhibitory DREADD reduced ARC cFOS immunolabelled neurons in fed mice (arrowheads). Representative images of four independent experiments (a–c). **d**, e, CNO-activated inhibitory DREADD blocked ACEA-induced POMC activation (cFOS; vehicle plus ACEA, $n = 6$ mice, $60.4 \pm 3.6\%$; CNO plus ACEA, $n = 5$, $32.3 \pm 2.5\%$; $***P < 0.001$). **f**, CNO-activated POMC-specific inhibitory DREADD did not acutely affect feeding but enhanced it after 8 h (vehicle, $n = 17$ mice, 0.42 ± 0.04 g; CNO,

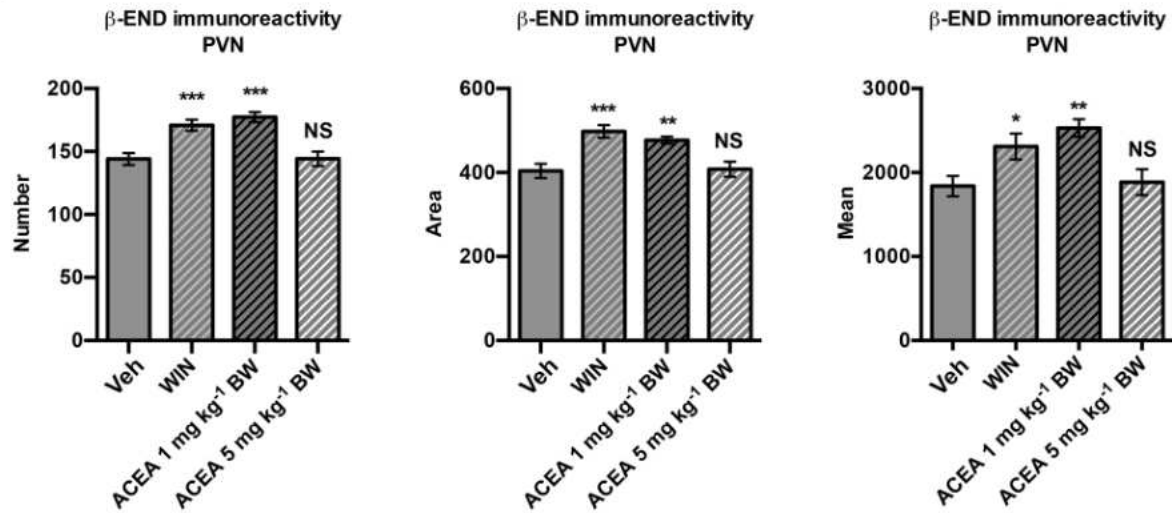
$n = 16$, 0.58 ± 0.04 g; 24 h after injection: vehicle, $n = 5$ mice, 2.57 ± 0.07 g; CNO, $n = 5$, 3.37 ± 0.18 g; $**P < 0.01$ versus vehicle; three independent experiments). **g**, CNO-activated POMC-specific stimulating DREADD did not acutely affect feeding but reduced it after 8 h (vehicle, $n = 6$ mice, 0.58 ± 0.05 g; CNO, $n = 6$, 0.34 ± 0.05 g; $**P < 0.01$ versus vehicle; 24 h after injection: vehicle, 3.96 ± 0.15 g; CNO, 3.65 ± 0.21 g; $P > 0.05$ versus vehicle). Values (biological replicates) denote mean \pm s.e.m. If not otherwise stated, P values (unpaired comparisons) by two-tailed Student's t -test. Scale bars, 100 μ m (a), 25 μ m (b) and 50 μ m (c, d).



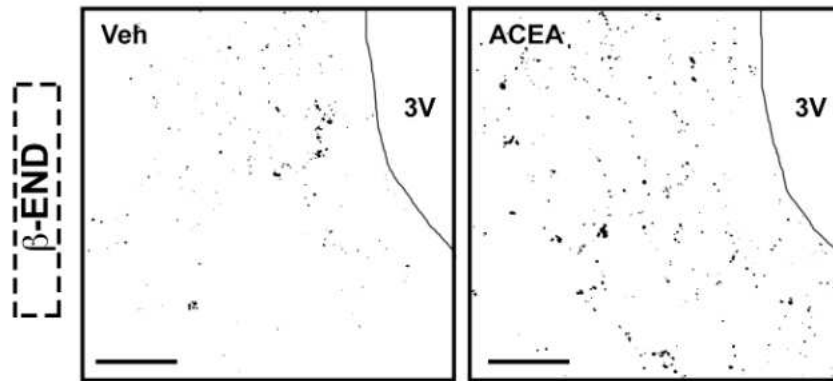
Extended Data Figure 3 | Hyperphagic CB_1R activation selectively increased PVN β -endorphin. a–d, i, PVN α -MSH remained unchanged after hyperphagic CB_1R activation (PVN unilateral analysis; vehicle, $n = 6$ values (technical replicates)/6 sections/3 mice (biological replicates); 60 min ACEA, $n = 10/10/5$; 90 min ACEA, $n = 6/6/3$; values, see Extended Data Table 1a). e–h, j, In contrast, hyperphagic ACEA increased PVN β -endorphin 60 and

90 min after application (PVN unilateral analysis; vehicle, $n = 13$ values/13 sections/6 mice; 60 min ACEA, $n = 4/4/4$; 90 min ACEA, $n = 14/14/7$; values, see Extended Data Table 1b. *** $P < 0.001$, * $P < 0.05$ versus vehicle, one-way ANOVA, followed by Dunnett's multiple comparisons test, two independent experiments using litters from different parents). Error bars indicate mean \pm s.e.m. Scale bars, 25 μ m.

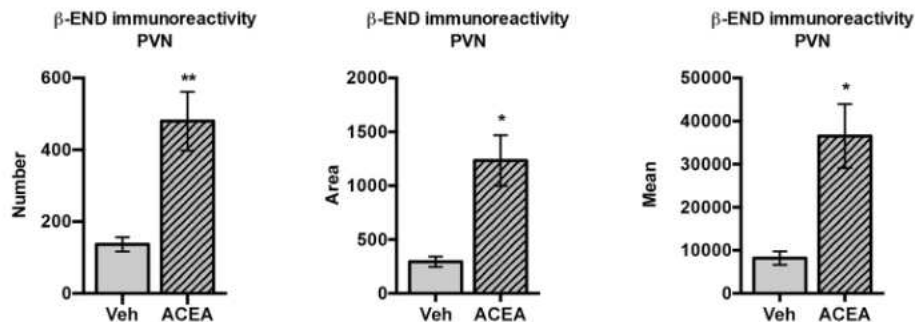
a



b

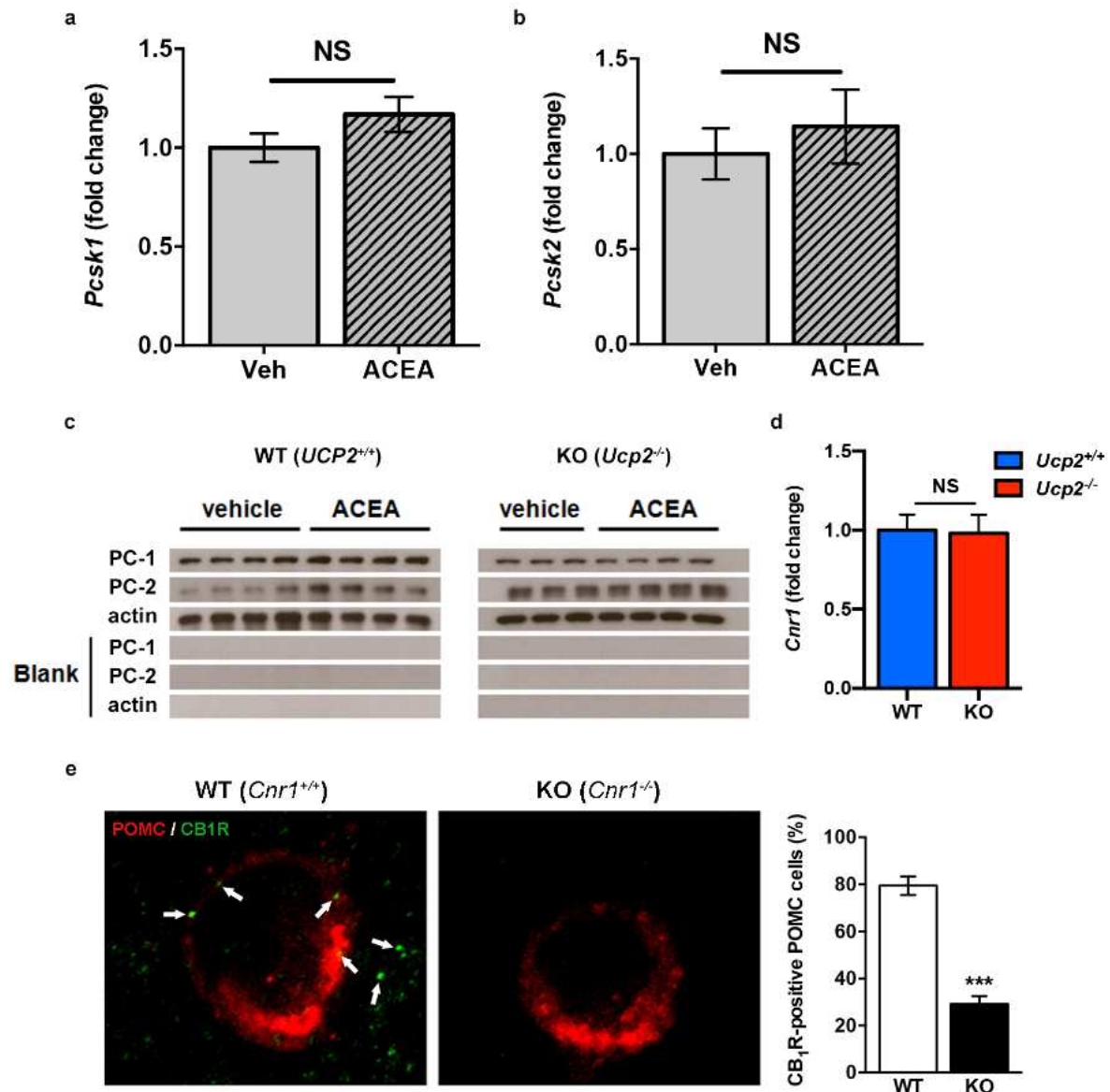


c



Extended Data Figure 4 | Bimodal character of ARC CB₁R-driven β -endorphin increase. **a**, Compared to vehicle (bilateral PVN analysis; $n = 22$ values (technical replicates)/11 sections/4 mice (biological replicates), hyperphagic doses (1 mg kg^{-1} body weight, respectively) of WIN ($n = 24/12/4$) or ACEA ($n = 18/9/3$) induced PVN β -endorphin immunoreactivity. Neutral dose (5 mg kg^{-1} BW) of ACEA ($n = 18/9/3$) on feeding showed no effects (see Extended Data Table 2 for all values). * $P < 0.05$, ** $P < 0.01$, *** $P < 0.001$ versus vehicle, one-way ANOVA, followed by Dunnett's multiple comparisons test. **b**, Representative binary images of four independent experiments

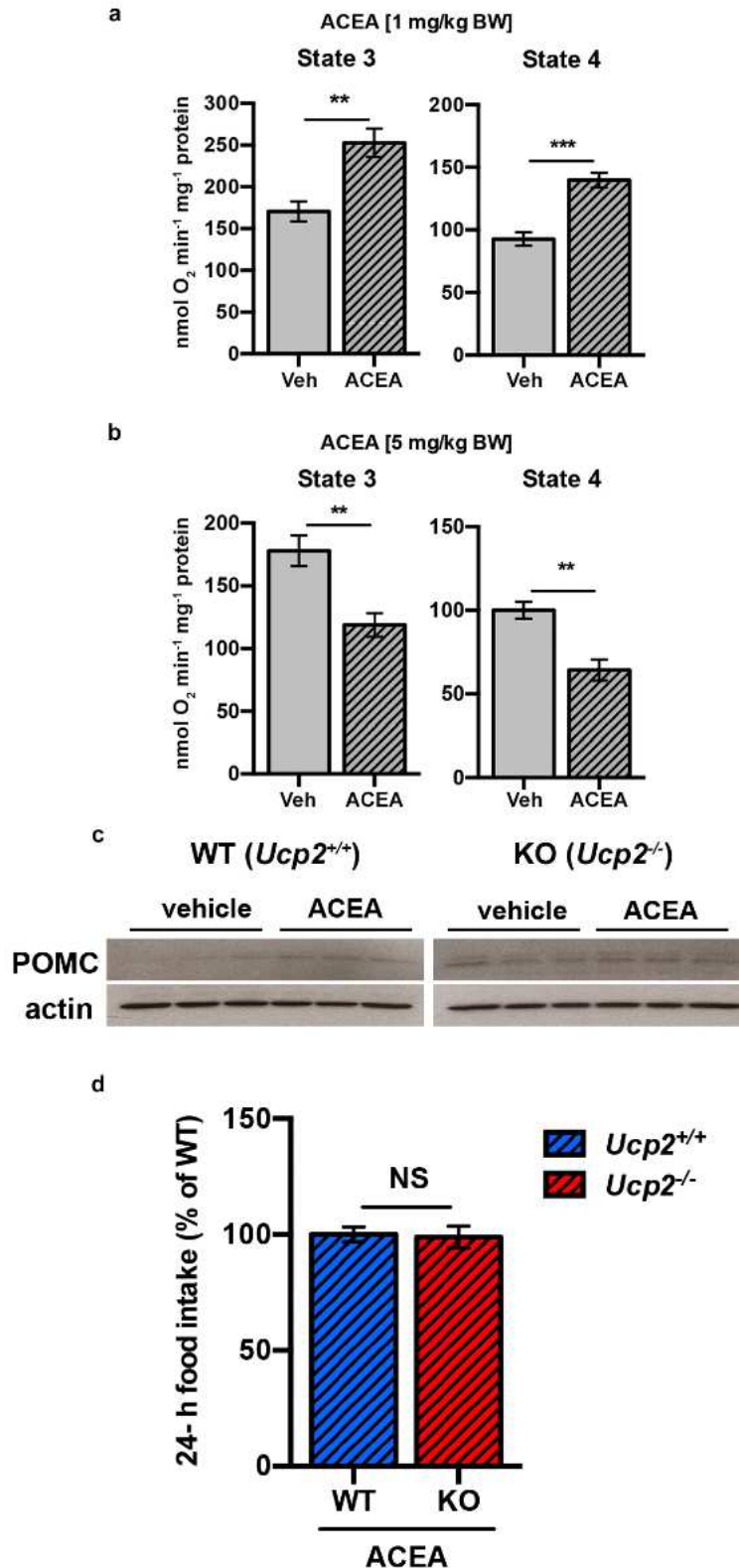
showing β -endorphin immunoreactivity after thresholding (image segmentation) using ImageJ software (see Methods). **c**, Compared to vehicle (unilateral PVN analysis; $n = 4$ mice (biological replicates), 2–3 sections (technical replicates) per mouse), central, hyperphagic local ARC injection of ACEA ($n = 5$ mice, 3 sections per mouse) increased PVN β -endorphin immunoreactivity (see Extended Data Table 3 for all values; * $P < 0.05$, ** $P < 0.01$). Error bars indicate mean \pm s.e.m. If not otherwise stated, P values (unpaired comparisons) by two-tailed Student's t -test. Scale bars, $100 \mu\text{m}$.



Extended Data Figure 5 | Post-transcriptional regulation of hypothalamic pro-protein convertases, normal *Cnr1* expression in *Ucp2^{-/-}* mice and presence of CB₁R in POMC neurons.

a, b, ACEA did not affect transcripts of pro-protein convertases 1 (*Pcsk1*) and 2 (*Pcsk2*) (in fold change; *Pcsk1*: vehicle, $n = 11$ mice, 1.00 ± 0.07 ; ACEA, $n = 10$ mice, 1.17 ± 0.09 ; *Pcsk2*: vehicle, $n = 11$ mice, 1.00 ± 0.13 ; ACEA, $n = 11$ mice, 1.14 ± 0.19 ; $P > 0.05$; two independent experiments). **c**, Representative western blot membranes for PC-1 (~80 kilodaltons (kDa)) and PC-2 (~72 kDa) immunolabelling. **d**, Equal *Cnr1* expression in wild-type and *Ucp2^{-/-}* mice (in fold change: all groups $n = 6$ mice; wild type, 1.00 ± 0.1 ; *Ucp2^{-/-}*, 0.98 ± 0.12 ; $P > 0.05$). **e**, We have previously shown that antibodies raised against CB₁R also recognized the mitochondrial protein, stomatin-like protein 2 (ref. 21). In line with this,

mitochondrial labelling of CB₁R was found substantially diminished but not completely eliminated in CB₁R-KO (*Cnr1^{-/-}*) mice²³⁻²⁵. We observed that in contrast to wild-type animals (*Cnr1^{+/+}* mice), which showed ~80% (77 out of 97, $79.5 \pm 3.9\%$) of POMC neurons (red fluorescence) to contain labelling with the CB₁R antisera (green fluorescence), in CB₁R knockout (KO; *Cnr1^{-/-}*) mice, less than 30% (37 out of 128, $29.2 \pm 3.3\%$) of POMC neurons retained immunolabelling. Thus, we concluded that a large population of POMC neurons contains CB₁R ($***P < 0.001$). All values (biological replicates: **a-c, d**; biological replicates including technical replicates: **e**) denote mean \pm s.e.m. If not otherwise stated, P values (unpaired comparisons) by two-tailed Student's *t*-test. Scale bar, 25 μ m.



Extended Data Figure 6 | Bimodal CB₁R-dependent regulation of mitochondrial respiration and UCP2-dependent control of POMC.

a, b, Bimodal CB₁R-controlled mitochondrial respiration in hippocampus. **a**, Hyperphagic (1 mg kg⁻¹ body weight ACEA, intraperitoneal) CB₁R activation increased *ex vivo* mitochondrial respiration (in nmol O₂ min⁻¹ mg⁻¹ protein; state 3: vehicle, *n* = 6 mice, 170.7 ± 12; ACEA, *n* = 8, 252.7 ± 17.2; state 4: vehicle, 92.7 ± 5.4; ACEA, 139.7 ± 6; ***P* < 0.01, ****P* < 0.001). **b**, Neutral dose of ACEA on feeding (5 mg kg⁻¹ body weight, intraperitoneal) reduced mitochondrial respiration (state 3: vehicle, *n* = 7 mice,

178.2 ± 12.2; ACEA, *n* = 5, 118.9 ± 9.4; state 4: vehicle, 100 ± 5.1; ACEA, 64.3 ± 6.3; two independent experiments). **c**, Representative western blot membranes for POMC (pre-POMC, ~31 kDa; POMC, ~27 kDa). **d**, The 24-h food intake did not differ between wild-type (*n* = 28 mice, 100 ± 3.2%) and *Ucp2*^{-/-} (*n* = 29, 98.9 ± 4.7%; *P* > 0.05) mice after ACEA (1 mg kg⁻¹ body weight, intraperitoneal) treatment (six independent experiments using litters from different parents). All values (biological replicates) denote ± s.e.m. If not otherwise stated, *P* values (unpaired comparisons) by two-tailed Student's *t*-test.

Extended Data Table 1 | Semi-quantitative measurements of α -MSH and β -endorphin immunoreactivity

a

α -MSH in PVN	Number	Area	Mean
Veh	277.5±21	392.9±30.4	41691±3627
60 min ACEA	235.5±34	327.1±56	33244±5291
90 min ACEA	284±26.5	377.6±41.3	39751±3861

b

β -END in PVN	Number	Area	Mean
Veh	134.9±12.4	289.9±28.2	8774±1048
60 min ACEA	348.5±44***	863.2±103.6***	18468±813.5***
90 min ACEA	203.1±19.5*	446.8±42.4*	12935±1362*

a, α -MSH immunoreactivity; see Extended Data Fig. 3a–d, i. b, β -endorphin immunoreactivity; see Extended Data Fig. 3e–h, j. ** $P < 0.01$, *** $P < 0.001$ versus vehicle.

Extended Data Table 2 | Semi-quantitative measurements of β -endorphin immunoreactivity

β -END in PVN	Number	Area	Mean
Veh	144 \pm 4.8	403.7 \pm 17.2	1838 \pm 121.4
90 min WIN (1 mg kg ⁻¹ BW)	170.8 \pm 4.4***	497.6 \pm 15.1***	2308 \pm 154.3
90 min ACEA (1 mg kg ⁻¹ BW)	177.3 \pm 3.9***	477 \pm 8.4**	2528 \pm 104.2
90 min ACEA (5 mg kg ⁻¹ BW)	144.2 \pm 5.7	407.9 \pm 17.9	1885 \pm 154.8

See Extended Data Fig. 4a. * P <0.05, ** P <0.01, *** P <0.001 versus vehicle.

Extended Data Table 3 | Semi-quantitative measurements of β -endorphin immunoreactivity

β-END in PVN	Number	Area	Mean
Veh	136.7\pm19.9	294.3. \pm47.7	8205\pm1550
60 min ACEA	480\pm81.6**	1235\pm235*	36526\pm7431*

See Extended Data Fig. 4c. * $P < 0.05$, ** $P < 0.01$ versus vehicle.

Extended Data Table 4 | Semi-quantitative measurements of β -endorphin immunoreactivity

β -END in PVN	Number	Area	Mean
WT - Veh	254.5 \pm 13.2	287.1 \pm 14.8	6885 \pm 352.7
WT - 90 min ACEA	311.9 \pm 22.6*	365.6 \pm 24.1**	8007 \pm 407.4*
<i>Ucp2</i> ^{-/-} - Veh	247.4 \pm 21.3	296 \pm 25.2	6840 \pm 478.3
<i>Ucp2</i> ^{-/-} -90 min ACEA	194.7 \pm 14.6*	224 \pm 16.9*	4849 \pm 328.2**

See Fig. 5j. * $P < 0.05$, ** $P < 0.01$ versus wild-type-vehicle or *Ucp2*^{-/-}-vehicle, respectively.